ACCSCIENCE PUBLISHING

International Journal of Bioprinting

REVIEW ARTICLE

Bioprinting of cell-laden protein-based hydrogels: From cartilage to bone tissue engineering

Mehran Khajehmohammadi[1,2†], Negar Bakhtiary[3†], Niyousha Davari[4], Soulmaz Sarkari[5], Hamidreza Tolabi[6,7], Dejian Li[8], Behafarid Ghalandari[9*], Baoqing Yu[10*], and Farnaz Ghorbani[11,12,13*]

[1]Department of Mechanical Engineering, Faculty of Engineering, Yazd University, Yazd 8174848351, Iran

[2]Medical Nanotechnology and Tissue Engineering Research Center, Yazd Reproductive Sciences Institute, Shahid Sadoughi University of Medical Sciences, Yazd 8916877391, Iran

[3]Department of Biomaterials, Faculty of Interdisciplinary Science and Technology, Tarbiat Modares University, Tehran 14115114, Iran

[4]Department of Life Science Engineering, Faculty of New Sciences and Technologies, University of Tehran, Tehran 143951561, Iran

[5]Department of Cardiology, School of Medicine and Health Sciences, Carl von Ossietzky University of Oldenburg, Oldenburg, Germany

[6]New Technologies Research Center (NTRC), Amirkabir University of Technology, Tehran 158754413, Iran

[7]Department of Biomedical Engineering, Amirkabir University of Technology (Tehran Polytechnic), Tehran 158754413, Iran

[8]Department of Orthopedics, Shanghai Pudong Hospital, Fudan University Pudong Medical Center, Shanghai, China

[9]State Key Laboratory of Oncogenes and Related Genes, Institute for Personalized Medicine, School of Biomedical Engineering, Shanghai Jiao Tong University, Shanghai 200030, China

[10]Department of Orthopedics, Shanghai Pudong New Area People's Hospital, Shanghai, China

[11]Department of Translational Health Sciences, University of Bristol, Bristol BS1 3NY, United Kingdom

[12]Institute of Biomaterials, Department of Material Science and Engineering, University of Erlangen-Nuremberg, Cauerstraße 6, 91058 Erlangen, Germany

[13]Institute of Orthopaedic and Musculoskeletal Science, Royal National Orthopaedic Hospital, University College London, London, United Kingdom

†These authors contributed equally to this work.

***Corresponding authors:**
Behafarid Ghalandari (behafarid.gh@gamil.com

Baoqing Yu (doctorybq@163.com)

Farnaz Ghorbani (farnaz.ghorbani@fau.de)

Citation: Khajehmohammadi M, Bakhtiary N, Davari N, et al., 2023, Bioprinting of cell-laden protein-based hydrogels: From cartilage to bone tissue engineering. *Int J Bioprint*, 9(6): 1089. https://doi.org/10.36922/ijb.1089

Received: June 16, 2023
Accepted: August 3, 2023
Published Online: September 7, 2023

(This article belongs to the *Special Issue: Advances in 3D Bioprinting for Regenerative Medicine and Drug Screening*)

Abstract

The fabrication of cell-laden protein-based hydrogels (PBHs) for bioprinting necessitates careful consideration of numerous factors to ensure optimal structure and functionality. Bioprinting techniques, such as single-cell, multi-cell, and cell aggregate bioprinting, are employed to encapsulate cells within PBHs bioink, enabling the creation of scaffolds for cartilage and bone regeneration. During the fabrication process, it is imperative to account for biophysical and biochemical factors that influence cell behavior and protein structure within the PBHs. Precise control of crosslinking methods, hydrogel rheological properties, and printing parameters is also crucial to achieve desired scaffold properties without compromising cell viability and protein integrity. This review primarily focuses on the influence of biophysical factors, including composition, microstructure,

biodegradation, and crosslinking, as well as biochemical factors, including chemical structure, growth factors, and signaling molecules, on protein structure and cell behavior. Additionally, key considerations for bioprinting PBHs and their impact on the successful regeneration of tissues are discussed. Furthermore, the review highlights current advancements, existing challenges, and promising prospects in the development of cell-laden PBHs for bioprinting applications and the regeneration of bone and cartilage.

Keywords: Bioprinting; Protein; Bioink; Cartilage; Bone; Tissue engineering

1. Introduction

The field of tissue engineering (TE) and regenerative medicine may undergo a revolution due to the development of bioprinting, a rapidly developing technology. An important application of bioprinting is in cartilage and bone TE, where it can be used to fabricate complex three-dimensional (3D) structures that mimic the structure and mechanical properties of natural tissues[1]. As a potential method for fabricating cartilage and bone tissue constructs, bioprinting of cell-laden protein-based hydrogels (PBHs) has emerged in recent years[2-4].

Traditional scaffolds cannot efficiently transport nutrients or exchange oxygen without porous structures interconnected in a complex geometry, and cells are typically deposited randomly using TE fabrication techniques[5,6]. In order to overcome these barriers, 3D bioprinting techniques can be used to construct cell-laden 3D structures[7,8]. By using cell-laden hydrogels, bioprinting makes tissue constructs with a high cell density, which plays a vital role in tissue regeneration. Bioprinting technology is divided into two distinct groups that are not mutually exclusive. Two basic categories can be distinguished: distributed versus aggregated cells and single versus multi-cellular. Cell aggregate bioprinting involves embedding preformed cell aggregates in bioinks and then printing them. Unlike single-cell bioprinting, which involves printing one cell at a time, multi-cell bioprinting involves suspending several cells in bioink and depositing them in a filament or droplet[9]. The incorporation of multiple cell types, such as chondrocytes and osteoblasts, into bioprinted osteochondral tissue constructs enhances the formation of a functional interface between cartilage and bone[10]. The fabrication of cartilage and bone tissue constructs has been achieved using multi-cell bioprinting technologies, including inkjet printing, extrusion-based printing, and laser-assisted printing. These technologies permit the fabrication of complex 3D structures with high reproducibility and shape fidelity[11-13].

Hydrogels are popularly employed as bioinks in the bioprinting process because of their chemical structure and the favorable 3D environments they provide for cellular growth[14-17]. Incorporating cells into inks (i.e., biomaterials or biological materials) to create a "bioink" is the cornerstone of producing intricate, biologically applicable 3D tissue structures[18,19]. The use of PBHs as bioinks for bioprinting has several advantages over other hydrogel systems. PBHs are biocompatible, biodegradable, and can be functionalized with cell adhesion peptides and growth factors (GFs) to enhance cell behavior and tissue regeneration[20,21]. Moreover, they can be crosslinked *in situ* by various mechanisms, such as physical, chemical, or enzymatic crosslinking, to achieve the desired mechanical properties and stability. In recent years, several PBHs have been developed for the bioprinting of cartilage and bone tissue constructs. These hydrogels offer several advantages over other materials, such as synthetic polymers or decellularized extracellular matrix (ECM) scaffolds. PBHs, such as collagen, gelatin, and fibrin, are biocompatible and biodegradable and can support cell adhesion, proliferation, and differentiation[22-24]. By providing spatial factors, such as porosity, protein alignment, and network density, the tissue structure can influence cellular behavior, shape, migration, and fate. Therefore, PBHs aim to replicate the ECM's complex and unique structure to develop functional tissue constructs that can mimic the native tissue's mechanical and biological properties[25-28]. The ability to imitate the native tissues' ECM and the tendency to experience shear-thinning before regaining their original shape are other desirable features of protein-based materials. Furthermore, protein-based polymers can be utilized to adjust the rheological and biochemical properties of bioinks, thereby enhancing the shape fidelity[29-32]. Further, these materials are renewable and green compared to fossil-derived synthetic polymers, and their availability and ease of large-scale production via bioengineering methodologies and biotechnological techniques make them attractive to researchers[33,34]. Thus far, more natural proteins of animal origin have been used in the fabrication of hydrogels, the reasons for which are easier access, lower cost, and simplicity of extraction, which will be followed by their introduction and review in the synthesis of biological inks for osteochondral and cartilage TE.

The protein sequence of hydrogels can significantly influence bioprinting processes and tissue constructs[35,36]. PBHs differ in terms of their mechanical properties, degradation rates, and cell adhesion properties, which can have a major impact on the printability of hydrogels and the behavior of cells. As an example, collagen hydrogels

are known for their biocompatibility and ability to support cell adhesion and proliferation, but their mechanical strength is low and they degrade rapidly. Although fibrin hydrogels have a higher mechanical strength and a slower degradation rate than collagen hydrogels, they may not promote cell adhesion and proliferation as well as collagen hydrogels[37-39]. The sequence and structure of proteins determine the stiffness, swelling, and degradation rate of hydrogels. As a consequence, it can influence the behavior of cells and the regeneration of tissue within bioprinted constructs[40-42]. Furthermore, specific functional groups or peptides may be introduced into protein sequences to enhance cell adhesion, differentiation, or tissue regeneration[43]. For example, arginine-glycine-aspartic acid (RGD) peptides are known to enhance cell adhesion and can be incorporated into the protein sequence of hydrogels in order to enhance biocompatibility and cell behavior[44]. Thus, it is necessary to carefully consider the protein sequence and structure of the hydrogel in order to optimize the mechanical and biological properties of the final tissue constructs.

This study aims to provide a comprehensive review of innovative bioprinting technologies, which are classified based on the cell format and the number of cells generated during the bioprinting procedure. The study focuses on PBHs utilized in cartilage and bone TE. Additionally, the critical role of microenvironmental factors, including biophysical and biochemical parameters, in bioprinting cell-laden PBHs is examined in detail, with reference to relevant research. The subsequent section provides a thorough explanation of the process compatibility considerations for PBHs, including mechano-rheological properties, biocompatibility, and process factors, through an overview of recent experiments on PBHs bioprinting. Finally, the challenges and perspectives associated with PBHs that must be carefully addressed to advance this fascinating field are highlighted.

2. Bioprinting strategies

There have been numerous developments within the bioprinting field to meet the needs of different research fields in terms of manufacturing capabilities, such as printing resolution, speed, or throughput[45], as well as cell requirements, including cell viability, proliferation, or differentiation[46]. It is possible to categorize the bioprinting technology into two distinct groups, which are not mutually exclusive. In essence, they can be classified based on the format of the cells (distributed cells or aggregated cells) and the number of cells produced during printing (single-cell or multi-cell). Single-cell bioprinting involves printing one cell at a time, while in multi-cell bioprinting, the cells are suspended in a bioink, and a number of cells are deposited within each filament or droplet. Within cell aggregate bioprinting, preformed cell aggregates are embedded into bioinks and then printed[9] (Figure 1).

The goal of single-cell bioprinting is to distribute single cells in a controlled manner in order to fabricate delicate tissues and study single cells genetically[47,48]. Particularly, the arrangement of cells and the microenvironment play a crucial role in stem cell research. There are several methods available for isolating and manipulating single cells as the first phase in the single-cell characterization[49]; to separate single cells, fluorescent-activated cell sorting (FACS)[50] and limiting dilution[51] are two widely used approaches[52]. Nevertheless, the inefficiency of limiting dilutions, together with the need for specialized instruments, as well as requiring professional expertise to employ FACS restrict their use[49,52]. Recent innovations in the field of single-cell printing have contributed to circumventing these limitations, one of which is utilizing a variety of microfluidic approaches for the encapsulation and examination of single cells, comprising droplet microfluidics[53-55], microwell arrays[56,57], and hydrodynamic traps[58,59]. Single-cell bioprinting offers multiple benefits; firstly, it enables precise and effective cell distribution at high throughput[60], and second, each cell or colony can be recovered readily with addressability for further analysis. Another advantage of single-cell printing is that it can easily be integrated with other methods, such as imaging systems[61,62], electric fields[63-65], and acoustic fields[66,67], with the encapsulation efficiency exceeding 90%. Based on Poisson's distribution, the broadly employed droplet-based microfluidics' theoretical limit is only 37%. Furthermore, single-cell printing can create both high-resolution two-dimensional (2D) structures as well as 3D tissue matrices for TE, drug delivery, and toxicology[68,69]. Barron *et al.*[70] first proposed the concept of single-cell bioprinting in 2005, when they described the bioprinting of human osteosarcoma cells, shortly after laser-assisted bioprinting was invented. To control the number of cells in a droplet, they developed bioinks with varying cell concentrations. Although the droplets were homogeneous and of small size, identifying only one cell per droplet was difficult, and the number of cells within the droplet generally followed the Poisson's distribution regardless of their concentration. Since then, single-cell bioprinting was not invented until 2012, when a camera with high speed was employed in order to monitor cells in the nozzle tip[71]. In this regard, droplets containing more than one cell or not incorporating any cells were discarded. It was in 2014 that Zhang *et al.*[72] developed a method to block cell-print breast cancer cells, utilizing traps with hook-shaped ends arranged in a prescribed pattern to capture and print singular cells. Currently, a variety of techniques

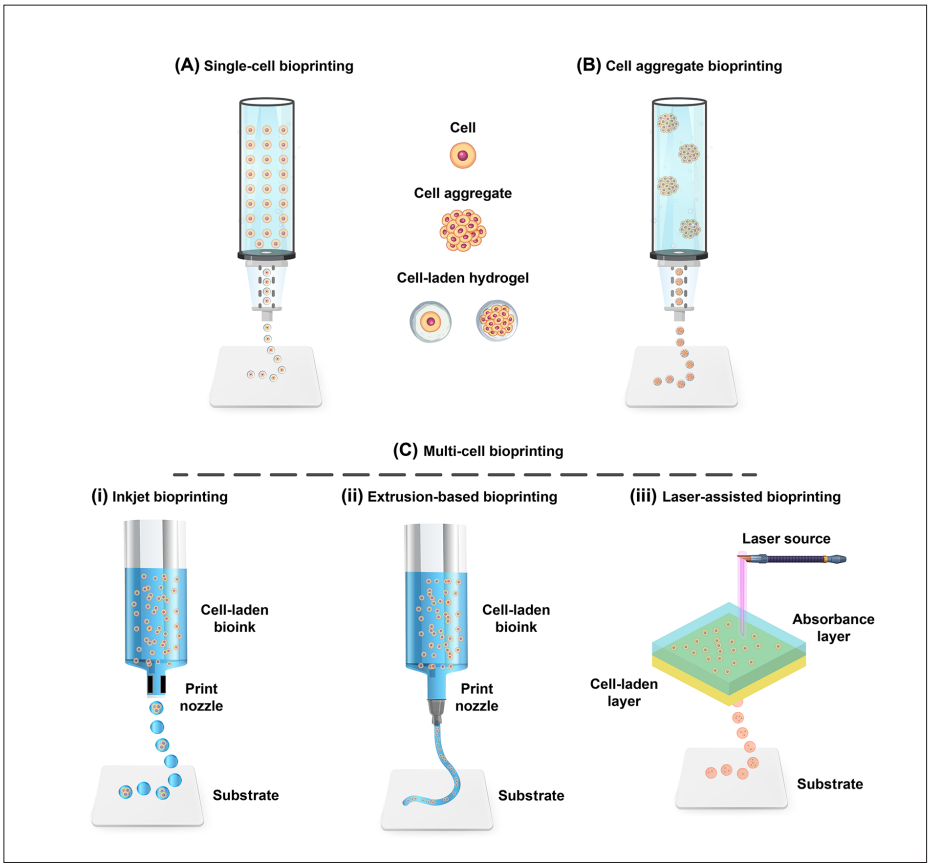

Figure 1. Illustrations of various bioprinting methods: (A) single-cell bioprinting, (B) cell aggregate bioprinting, and (C) multi-cell bioprinting, which can be further divided into (i) inkjet bioprinting, (ii) extrusion-based bioprinting, and (iii) laser-assisted bioprinting.

for single-cell printing are available, consisting of acoustic field-based printing or label-free computer vision-based printing[73]. In spite of the fact that stem cell bioprinting using single-cell methods has not been demonstrated to date, single-cell research employing stem cell bioprinting techniques is clearly on the rise, indicating the importance of stem cell biology. The current state of 3D printing does not allow the printing of organs and tissues with single-cell resolution, that is of necessity for printing functional organs and tissues[68,69,74,75].

Cell aggregate bioprinting is replicating the structure and function of tissues by utilizing the properties of aggregated cells[76]. Since aggregated cells have a greater number of cell–cell contacts and a decreased number of cell–substrate contacts, aggregated cells experience a different microenvironment in comparison with single cells. Cell aggregate bioprinting, on the other hand, has much higher throughput because each aggregate consists of 500 to 250,000 cells[77]; as a result, this technique is of significant importance in the regeneration of large quantities of tissue. The bioprinting process of cell aggregates involves the formation of cell aggregates, their bioprinting, and their fusion and maturation. Several methods can be employed to create cell aggregates through self-assembly and self-organization, including hanging drop culture, scaffolds, non-adhesive surfaces, and microfabrication[78], capable of generating sheets[79], spheroids, and cylinders[80]. Cell aggregate bioprinting requires proper mechanical stability to prevent fractures during bioprinting and long-term culture; thus, choosing cells for this bioprinting approach is of high significance. Different printing methods are utilized to create cell aggregates that are mainly categorized according to the contact between the cell and the substrate. In the first technique, bioactive bioinks are used to encapsulate cell aggregates and provide adhesion ligands[81]. As the second method, scaffold-free bioprinting refers to co-printing bioinert materials with cell aggregates[82]. Initially, cell aggregates form adjacently without any surrounding materials, and bioinks merely serve as supports until the aggregates fuse and form a tissue that is stable enough to stand on its own. After bioprinting, it is essential to rapidly fuse cell aggregates together in order to build stable tissues[9]. Since cell aggregates are the building blocks of a printed structure, enhancing inter-aggregate force through aggregate fusion contributes to

the structure's stability[80]. The mechanism is thought to be controlled via cell interactions and migrations, which is analyzed in some cases by means of phase field theory[83,84]. Besides, cell aggregate maturation is a crucial step; in fact, changing the microenvironment in cell aggregates simulates tissue formation *in vivo* to accelerate maturation and generate stable, functional tissues[85].

In multi-cell bioprinting, subdivided into inkjet bioprinting, extrusion-based bioprinting, and laser-assisted bioprinting[86], cells are suspended in hydrogels called bioinks[87]. Employing this approach, cells are printed randomly according to their concentration percentage in the bioink, and a scaffold is created afterward[88]. Inkjet printing is based on the deposition of bioink drops in a predetermined way to create a final multi-layer pattern. As a result of thermal or piezoelectric changes, pressure pulses generate drops with a defined volume in the range of picoliters. Commercial thermal printers utilize heating elements to expel ink droplets and form vapor bubbles that are heated to 300°C for a few microseconds. Printing on a substrate in the Z-direction is possible with a micropositioning stage[25]. Despite possessing a relatively low printing resolution, this printing process provides rapid scaffold production at an affordable cost. Of note, low-viscosity materials and low cell concentrations should be used to avoid nozzle clogging[89]. Extrusion-based bioprinters disperse bioinks as strands via a screw plunger or an air pump; to be more specific, the dispenser is mounted on a robotic stage, enabling the printing head to move in three directions. As a result of their design, extrusion-based bioprinters can be used with hydrogels having different viscosities and cell densities, and compared with inkjet-based bioprinting, there is less risk of clogging. However, if viscous hydrogels are utilized, a longer printing time and higher mechanical stresses may reduce the viability of encapsulated cells by 40–80%[90]. In laser-based bioprinting, the bioink is transferred from one substrate to another; to elucidate, pulses of the laser beam are responsible for this transfer, and in order to control the transfer of energy, a thin layer of energy-absorbing material (typically titanium or gold) is deposited on top of the donor substrate. In response to the absorption of energy, bioink droplets of defined sizes are formed. Although this technique is capable of printing materials with high viscosities and high cell densities at extremely high resolutions, it is limited by its excessive cost and inability to print large constructs[25]. In this regard, a number of TE projects have been successfully performed using the multi-cell bioprinting method[91-98]. Compared to cell aggregate and single-cell bioprinting, Table 1 summarizes the benefits and drawbacks of this method.

In summary, selecting the appropriate bioprinting technique requires consideration of both the fabrication process and the cell requirements. Bioprinting of cell aggregates is often necessary to produce large tissues in size or have tight junctions between cells. The use of single-cell bioprinting permits researchers to deposit microenvironment components and stem cells in precisely defined locations to study cell–matrix interactions. In contrast, multi-cell bioprinting has proven to be the most extensively used and advanced technique among all, for PBHs in particular.

3. Microenvironmental factors on bioprinting the cell-laden PBHs

In bioink formulation, it is crucial to consider the main material and concentration as key parameters in order to ensure the process's reproducibility and enhance printability. Natural structural proteins, such as collagen, elastin, silk fibroin, and fibrin, are particularly noteworthy for their physiological and biological cues, contributing to the development of bioinks. Additionally, PBHs are environmental friendly, renewable, and tend to exhibit excellent biocompatibility, strength, elongation, toughness, and slow degradability. All these remarkable materials' characteristics originate from the proteins' structure. Indeed, features of proteins, such as hydrophobicity and bioactivity, which are the building units of living organisms, depend on the amino acid constituents that are at the primary level, resulting in the folding of secondary

Tables 1. Benefits and drawbacks of different bioprinting techniques based on the format of the cells and the number of cells produced during printing

Bioprinting technique	Printing speed	Printing throughput	Resolution	Cell viability	Cell density	Cost
Single-cell	High	Low	High	Medium	Low	High
Cell aggregate	Medium	High	Low	High	High	Medium
Multi-cell						
Inkjet	High	Medium	Medium	Medium	Low	Low
Extrusion-based	Low	High	Low	Medium	High	Low
Laser-assisted	Medium	Medium	High	High	Medium	High

structures into the tertiary 3D configuration. Notably, proteins have functional amino and carboxyl groups that can be utilized to convert these materials into hydrogels by enzymatic, chemical, and physical crosslinking methods. The unfolding of protein and its accumulation into a gel matrix is the most frequent process in protein gelation, leading to alterations in conformation from the third to the second structure and the subsequent rise in random coil content. Specifically, the structural changes in proteins for the PBHs' formation are owing to the secondary structure content's alterations, and proteins' carboxyl and amino groups can form a hydrophilic environment, resulting in an inherent, great swelling property of PBHs[21]. One crucial factor in the bioprinting of PBHs is the hydrogel's mechanical characteristics specified via its network structure and crosslinking density. Generally, β-sheet structures are known to provide hydrogels with more robust mechanical features than α-helix structures due to their higher degree of crosslinking and stability; therefore, a greater content of β-sheet structures in PBHs can make them more suitable for bioprinting. As an instance, a group of researchers[99] performed the gelatin-silk fibroin bioink gelation employing enzymatic and physical crosslinking; to elucidate, the physical crosslinking (sonication) could accelerate the silk fibroin macromolecules' self-assembly in β-sheet crystals, which in turn improved the bioink rheology.

Physical and chemical factors are essential for the bioprinting process, especially the bioprinting of cell-laden PBHs. In this case, cells are incorporated into PBHs, and the microenvironment may affect the protein structures. For example, remodeling of the initial hydrogel matrix can happen as a function of incorporating the cells and secretion of native ECM[100]. Besides, hydrogel degradation and swelling can impact the bioprinted construct's integrity[101]. Thus, careful consideration should be given to several important biophysical cues, such as composition, biodegradation, porosity-related parameters, and crosslinking process. Furthermore, chemical structure, the presence of GFs and signaling molecules, as well as cell signaling, must be taken into account in the case of biochemical cues. All in all, the PBHs should meet several biophysical and biochemical requirements to be applied in bioprinting (Figure 2).

3.1. Biophysical factors

3.1.1. Composition

One of the most significant biophysical cues is the composition of PBHs, which must be taken into account when employing them as bioinks for cartilage and bone TE. In this regard, several aspects must be considered; firstly, PBHs must be innately non-immunogenic, non-cytotoxic, and minimally pro-inflammatory to ensure the health of cells[102]. Gelatin and collagen hydrogels are the most commonly employed PBHs for cartilage and bone regeneration due to their excellent biocompatibility and desirable capability to support cell growth and differentiation in these tissues[103]. In the case of PBHs, gelatin molecules are able to form partial triple-helical conformations by hydrogen bonds below a critical temperature, resulting in a sol-gel transition; however,

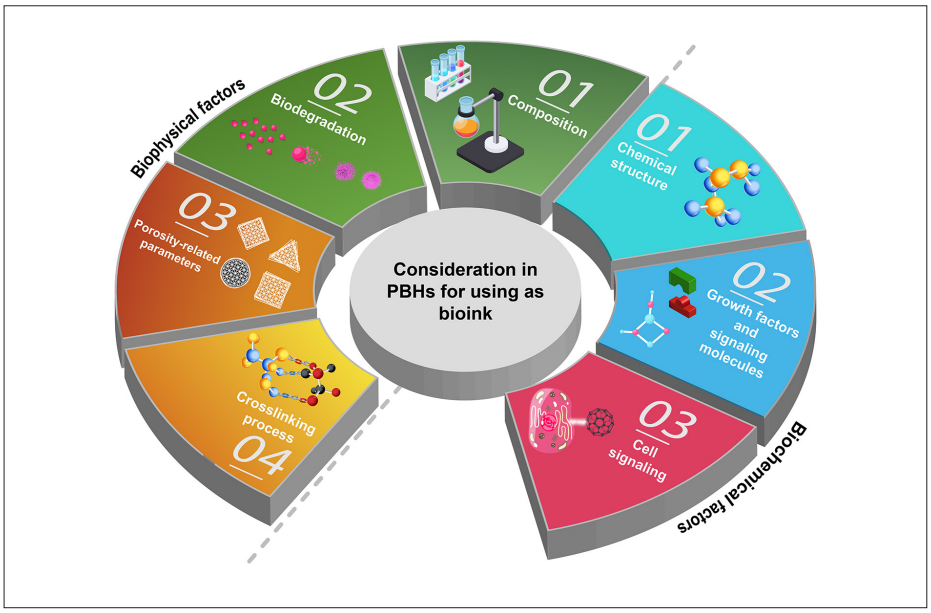

Figure 2. An overview of biophysical and biochemical considerations for the use of PBHs as bioinks.

beyond this temperature, hydrogen bonds weaken, and the helices disappear, leading to a gel-sol transition. As a result of this well-defined feature, gelatin has proven to be a versatile additive for the formulation of a wide variety of composite PBHs. Analogous to gelatin, collagen can also form gels at different temperatures and pH levels[104,105]. Compared with native tissues, its secondary helical conformation initiates a sol-gel transition for bioprinting but can commonly cause mechanical weakness. Hence, the molecular assembly of collagen is not controlled sufficiently, and therefore, native structural hierarchy is not present[106]. Moreover, fibrin and silk fibroin hydrogels display favorable outcomes and have unique advantages in certain applications, including ease of preparation and manipulation for fibrin and superior toughness and thermal stability for silk fibroin[107-110]. Secondly, PBHs should have appropriate mechanical features, especially elastic stiffness, which facilitate mechanical signaling to the cells for guiding differentiation, proliferation, and ECM deposition[102]. In the case of stiffness, bioinks with high stiffness or rigidity can inhibit the movement, growth, and differentiation of cells, whereas those with high softness are able to provide sufficient support for the encapsulated cells[111-113]. Concerning these subjects, a team of scientists[114] optimized the mechanical stiffness of alginate/gelatin bioinks (crosslinking approach: ionic crosslinking with 2% w/v $CaCl_2$ for 10 min) so as to improve ECM mineralization and cell organization for bone TE. With the aid of extrusion bioprinting, alginate/gelatin bioinks (4.1% w/v for gelatin and 0.8% as well as 1.8% w/v for alginate) loaded with P3 human mesenchymal stem cells (hMSCs) (cell density: 1.67×10^6, 5×10^6, and 15×10^6 cells/mL) having various stiffness were printed. They illustrated that soft scaffolds (0.8% w/v alginate, stiffness: 0.66 ± 0.08 kPa) possessed higher content of deoxyribonucleic acid (DNA) at day 28, enhanced expression of collagen type I alpha-II (6.7-fold increment from day 1 to day 28), increased alkaline phosphatase (ALP) activity at day 28, and stimulated osteogenic differentiation in comparison with the stiff ones (1.8% w/v alginate, 5.4 ± 1.2 kPa). Moreover, considerably less mineralized tissue was formed in stiff constructs than in soft ones at day 42 (22.6 ± 6.0 mm^3 versus 43.5 ± 7.1 mm^3) (Figure 3A). The mineral formation rate in the soft bioprinted scaffold was significantly higher than the stiff one at days 28–35 and 35–42. Interestingly, cells in soft scaffolds displayed a 3D cellular network in the mineralized matrix and osteoblast- and early osteocyte-related gene expressions at day 42. Within a pioneering investigation, Martyniak *et al.*[115] developed gelatin methacryloyl (GelMA)/hyaluronic acid methacrylate (HAMA) bioinks (crosslinking approach: photo-crosslinking with 0.05% w/v lithium phenyl-2,4,6-trimethylbenzoylphosphinate [LAP] at 405 nm wavelength and exposure times of 15, 38, and 60 s) and determined their ideal combination in the case of optimal stiffness for cartilage bioengineering. Human chondrocyte collagen type II–alpha-I–Gaussia luciferase reporter system (HuCol2gLuc) (cell density: 2×10^6 cells/mL) were embedded within the GelMA/HAMA bioink (15% w/v and 2% w/v), and the bioink was printed utilizing a pneumatic extrusion printing device. It was revealed that the HAMA addition to GelMA enhanced chondrogenesis, compared to GelMA (15% w/v) alone. Two ratios of GelMA/HAMA bioinks (1:1 and 2:1) with different stiffness (32 and 57.9 kPa) were assessed for cellular mobility and survival. High cellular viability (≥ 90%) was achieved for both bioprinted materials on all days. Furthermore, the GelMA/HAMA bioink with 1:1 ratio had considerably more fluorescent-labeled mobile cells (~2.5) compared to the 2:1 one (~1), and the cells also moved further (~26 μm) and faster (~1 μm/min) in the 1:1 ratio. All in all, the softer printed construct (1:1) showed a higher level of cellular mobility compared with the stiffer one (2:1). Notably, if multiple kinds of cell are contained in the PBHs, the characteristics of the PBHs should possess tenability to accommodate the various cellular requirements and allow spatiotemporal control if required.

3.1.2. Biodegradation

Bioinks that degrade too rapidly cannot provide adequate mechanical stability for long-term tissue development, while those that degrade too slowly may hinder tissue growth and ECM remodeling. In addition to being an essential feature for ECM deposition, PBHs' optimal degradation is indeed necessary for cell proliferation and mobility in the gel as well as the nearby host tissue[116]. In order to prolong the degradation rate of GelMA hydrogel, glycidyl-methacrylated HA (GMHA) was introduced into this system to obtain a novel bioink with a suitable degradation rate for cartilage regeneration applications. Employing extrusion bioprinting, GelMA/GMHA bioinks (crosslinking approach: photo-crosslinking with 0.03% w/v LAP) with various concentrations (7% w/v for GelMA and 3% and 5% w/v for GMHA) encapsulating tonsil-derived MSCs (cell density: 10×10^6 cells/mL) were printed, and the achieved constructs were subcutaneously implanted into female Bagg albino (BALB)/c nude mice models so as to observe the hydrogels' degradation characteristics after 3 weeks. It was illustrated that the 7% GelMA/5% GMHA-printed scaffold was fairly stable within the physiological environment and preserved its shape well with a low rate of degradation, allowing for tonsil-derived MSCs' chondrogenesis. Cells had high viability in the implanted hydrogel, and cartilage-like tissues, that were regenerated over time, could be observed. Furthermore, enhanced expression of collagen type II and formed hyaline matrices

demonstrating the bone matrix were seen 3 weeks post-implantation[117]. Another study in the field of cartilage TE evaluated the degradation of polyethylene glycol diacrylate (PEGDA)/gelatin/silk methacrylate (SilMA) bioink (crosslinking approach: photo-crosslinking with 0.2 w/v LAP at 405 nm wavelength, light-emitting diode (LED) light intensity 1000 mW/cm, and exposure time of 20 s) (6%, 9%, and 3% w/v) encapsulating primary porcine chondrocytes (cell density: 2×10^6 cells/mL) printed using extrusion-based printing and reported that delay in the degradation rate was seen after adding PEGDA to the composition, which was suitable for the load-bearing cartilage repair. Specifically, 90% degradation and minimal degradation of the printed hydrogel were observed after 28 days when incubating in protease enzyme and phosphate-buffered saline solution, respectively[118]. In the case of bone regeneration, an innovative experiment on the digital light processing (DLP)-based bioprinting of MC3T3-E1 preosteoblasts-encapsulated SilMA bioinks (crosslinking approach: photo-crosslinking with 0.2% wt LAP at 405 nm wavelength, visible blue light, and exposure time of 13 s for each layer) (cell density: 2×10^6 cells/mL) revealed that between three groups of 10%, 15%, and 25% w/v SilMA scaffolds with degradation percentages of 91.0 ± 2.27%, 64.8 ± 3.2%, and 48.6 ± 2.15% at 21 days, the 15% SilMA construct was the most efficient among the others in supporting the proliferation and attachment of the embedded cells[119].

3.1.3. Porosity-related parameters

Porosity-related parameters associated with bioprinted protein-based structures can affect *in vitro* cellular behaviors, in addition to *in vivo* tissue development[120]. Specifically, the presence of a porous structure into a printed scaffold is necessary for the diffusion of nutrients, cellular viability, cell migration, and proliferation, as well as *in vivo* tissue regeneration[121]. Utilizing cell-laden porcine tendon-derived collagen bioinks (1%, 3%, and 5% wt), porous collagen scaffolds crosslinked via genipin were printed and compared with non-porous ones, both fabricated via an extrusion printing system. Mostly live rabbit articular chondrocytes (cell density: 1×10^6 cells/mL) were found in the porous constructs' cross-sectional live and dead image, whereas dead cells were mostly present in the non-porous scaffolds' core after 7 days of cultivation. Indeed, the death of cells could be owing to the restricted nutrition penetrability of the collagen and the lack of a porous structure to compensate for this limitation. Notably, female New Zealand White rabbits with osteochondral defects were used as animal models, and the porous bioprinted collagen scaffold-treated group displayed significantly improved *in vivo* regeneration of cartilage, possessed newly-formed hyaline cartilage integrating well with the nearby cartilage, and showed high levels of glycosaminoglycans (GAGs) distribution compared to the non-porous scaffold-treated group having severe irregularity in the articular surface and defect lesions with centers that were not regenerated 4 weeks post-implantation[121]. Multiple evaluations have revealed that *in vivo* printed scaffolds with pore sizes of approximately 300 μm promote osteogenesis because of their higher permeability and capacity for vascularization; on the other hand, smaller pore sizes around 100 μm are more favorable for chondrogenesis[122]. Moreover, a porosity gradient in the radial direction can be found in the structure of bone, in which the mean porosity is enhanced from the cortical bone toward the trabecular bone[123,124]. To mimic this unique structure, a novel experiment employed DLP-based bioprinting system including a microfluidic mixer chip to print hMSCs-loaded 10% wt GelMA bioinks mixed with 10% wt GelMA solution comprising the porogen (crosslinking approach: photo-crosslinking with 2.20×10^{-3} M Tris(2,2-bipyridyl) dichlororuthenium (II) hexahydrate [Ru]/sodium persulfate [SPS] at 450 nm wavelength, blue light, and exposure time of 30 or 60 s for each layer) (cell density: 2×10^6 cells/mL). The final printed construct was three gradual zones featuring various pore sizes (12, 29, and 65 μm). Further tests illustrated the improved spreading of the encapsulated cells within the portions with larger pore sizes 7 days post-bioprinting. In comparison with the hydrogel segment that was mixed with 0.5% wt porogen, the cell cluster sizes were promoted to 2.5-fold and 4-fold in the gel regions containing 1.5% and 3.0% wt porogen, respectively. Thereafter, bone morphogenetic protein-2 (BMP-2) was integrated within the bioink in order to enhance the hMSCs' osteogenesis. The growth of MSCs, as cell clusters, filled in the pore areas and enhanced cell proliferation in portions having higher porogen concentration were observed, and improved expression of runt-related transcription factor 2 (RUNX2) (an osteoprogenitor in early stages) in the regions with larger pores and higher GF concentrations was confirmed[125].

3.1.4. Crosslinking process

The crosslinking process is another biophysical cue influencing the behaviors of encapsulated cells in the PBHs. For crosslinking of PBHs, physical, chemical, and enzymatic crosslinking approaches can be employed. Importantly, the crosslinker itself, its concentration, and the time of crosslinking affect the mechanical features of printed constructs and embedded cell properties[126-128]. Physical crosslinking involves using temperature or pH to form reversible interactions within the protein structure, influencing cell viability due to the sensitivity of cells to changes in temperature and pH. Furthermore, chemical crosslinking utilizes chemical agents to create covalent

bonds between protein molecules, resulting in the formation of a stable hydrogel structure; however, some chemical crosslinking agents can be toxic to cells and adversely affect cellular behaviors. Enzymatic crosslinking involves the employment of enzymes to catalyze the formation of crosslinks within the hydrogel, an approach that is biocompatible and offers more control over the crosslinking process. Nonetheless, enzymatic crosslinking requires longer incubation times, and the used enzymes need to be carefully handled to maintain cell survival. To be more specific, the chemically crosslinked network providing physical support impacts the stiffness and mechanical characteristics of the hydrogel; thus, breaking the chemical crosslinking bonds makes the PBHs more deformable and softer. Since embedded cells are able to sense and respond to the surrounding environment's mechanical properties, they experience alterations in their behaviors[129]. In the case of physical crosslinking, the crosslinks are usually reversible and can be broken via altering the pH, temperature, or ionic strength of the environment. Consequently, breaking these formed bonds can result in the dissolution of hydrogel or the loss of its structure; these phenomena exert effects on the encapsulated cells' organization, distribution, and survival[130–132]. Koo *et al.*[121] assessed the concentration and time effects of genipin, as a chemical crosslinker, on cell-laden collagen-based printed scaffolds' mechanical features and encapsulated rabbit articular chondrocytes' behaviors. In this regard, these scaffolds bioprinted by extrusion printing were dipped into the genipin solution having concentrations of 0.1, 1, and 5 mM in the culture medium for various times (0.5, 1, and 6 h). It was revealed that the cell-laden construct crosslinked with a higher concentration of genipin and longer crosslinking time displayed higher compressive modulus. Moreover, the compressive modulus enhanced with the increment of crosslinking agent's concentration and crosslinking time. At the crosslinker concentration of 0.1 mM, all of the cellular survival values at the crosslinking times of 0.5, 1, and 6 h were > 90% after 1 day of cultivation, and they even augmented up to 98 ± 0.4% after 7 days. At 1 mM concentration of genipin, the cellular viability gradually diminished by the crosslinking time's extension from 0.5 to 6 h, and the percentages of cell survival with the crosslinking time of 1 h were 88 ± 2.0% and 80 ± 0.5% at 1 and 7 days of cultivation, respectively. Nonetheless, at the higher genipin concentration of 5 mM, the viability of cells was decreased dramatically after 7 days due to the high genipin's concentration toxic effect or the excessively high compressive modulus via the immoderate cross-linking, which could fix the cells within the collagen strut and ultimately interrupt their metabolic activities. The scaffolds' controllability was also specified by lifting one of their sides so as to see if they could be readily handled for additional treatments like *in vivo* implantation; all of them except for the ones crosslinked with 0.1 mM genipin showed adequate controllability without the deformation of structure.

Among these constructs, only scaffolds that were crosslinked with genipin having 1 mM concentration and crosslinking time of 1 h possessed an average cell survival rate of 84%; as a result, these conditions were opted as the optimal crosslinking circumstances. Within a pioneering investigation that employed extrusion printing, scientists[133] reported the impacts of the tannic acid (TA), as chemical crosslinking agent used post-printing, with various concentrations (0.1%, 0.25%, 0.5%, 1%, and 3% wt) in the MC3T3-E1 preosteoblasts-embedded porcine tendon-derived collagen type I scaffolds (5% wt of collagen) (cell density: 5×10^6 cells/mL) on their physical characteristics and cellular activities. They set the crosslinking time to 10 min in order to impede high cell fixation which could disturb cellular activities. The scaffolds crosslinked with 0.1% and 0.25% wt crosslinker did not possess sufficient mechanical stability; indeed, they were not capable of preserving their original shape and readily bending around a steel rod. However, the concentration above 0.5% wt considerably enhanced the constructs' stability, and the structures could maintain their flat shape with mechanical strength. Compared with the cell-laden collagen constructs without crosslinking, the crosslinked ones had significantly improved mechanical properties. Furthermore, from concentration of 0.5% wt and above, the mechanical strength exponentially augmented (Young's modulus = 9.81 ± 0.88, 23.34 ± 1.84, and 67.13 ± 6.52 kPa for TA-0.5, TA-1, and TA-3 samples, respectively). Interestingly, non-crosslinked scaffolds had nearly 97% of degradation rate in 6 h, whereas the other crosslinked ones displayed relatively slow rate of degradation. During 10 days of observation, the degradation rate of the structures diminished with the increase of TA concentration as anticipated. In the case of cell behaviors, a minor decrease in cellular viability was seen from TA concentrations above 1% wt. Nevertheless, all scaffolds preserved great survival of cells (approximately 95–96%); to elucidate, the high viability with different TA concentrations demonstrated that the TA crosslinking process was totally safe for the MC3T3-E1 preosteoblasts. Cells initiated proliferation on T-0.1 and T-0.25 structures from day 4, and those on the T-0.5 scaffold could start at day 7. Thereafter, each of these systems exhibited significantly enhanced DNA expression. However, the T-1 scaffold did not display a significant difference in the values of DNA expression during 14 days of cultivation. The release of cells was noticeably high for the T-0.1 construct because of the low TA concentration

leading to the weaker crosslinking, while for the other crosslinked ones, the cell release was deterred from the strut owing to the stronger crosslinking. Among those constructs with controllability (T-0.5 and T-1 ones), the T-0.5 scaffold with better cellular behaviors was chosen as the optimum scaffold for further analyses in future studies. Table 2 summarizes the biophysical parameters influencing PBHs' bioprinting in the cartilage and bone TE.

3.2. Biochemical factors

3.2.1. Chemical structure

Cells' behaviors are impacted by diverse signals they receive from the ECM and neighboring cells; indeed, these received signals are capable of promoting adherence, morphogenesis, differentiation, and proliferation of cells[134]. Regarding the chemical structure as a biochemical cue, proteins in bioinks can exert effects in various ways, one of which is that they are able to promote cell spreading, survival, proliferation, and adhesion to the hydrogel matrix via presenting adhesive sites and specific ligands like matrix metalloproteinase (MMP) sequence and RGD sequence, which bind to the integrin receptors on cells surface[135]. Concerning this matter, cross-linker-free gelatin/silk fibroin bioinks (1.5% and 7% w/v) encapsulating primary chondrocytes (cell density: 10^6 cells/mL) for the cartilage TE were printed by employing an extrusion printing approach. They revealed enhanced cellular viability, improved cell adhesion, and increased ECM formation compared to the control group, which could be attributed to the RGD presence in both silk fibroin and gelatin proteins. Moreover, improved printability due to the shear-thinning behavior of silk and the high viscosity of gelatin was achieved[136]. Özenler *et al.*[137] designed mouse MC3T3-E1 preosteoblasts-loaded sodium alginate dialdehyde/gelatin bioinks (7.5% and 15% w/v) containing fish scale (FS) particles (1%, 3%, 5%, and 10% w/v) (cell density: 5×10^6 cells/mL) for bone regeneration. Then, they printed the bioinks using extrusion printing device and physically and chemically crosslinked the structures employing $CaCl_2$ and microbial transglutaminase, respectively (Figure 3B). As one of the results, the promotion of cellular proliferation during 28 days of cultivation was reported due to the gelatin's favorable RGD sequence. Another investigation developed arch-like bioprinted constructs utilizing GelMA and silk fibroin/gelatin bioinks (crosslinking approaches: photo-crosslinking with 0.25% w/v LAP at 365 nm wavelength (ultraviolet [UV] light with 700 mA) and exposure time of 2 min as well as enzymatic crosslinking with mushroom tyrosinase (800 units/mL), respectively) for cartilage regeneration. Employing extrusion printing, two compositions of bioinks (GelMA bioink: 10% w/v of GelMA and silk fibroin/gelatin bioink: 80 mg of gelatin powder from porcine skin type A in 800 μL of silk fibroin solution) loaded with human bone marrow-derived MSCs (hBMSCs) (cell density: 1×10^7 cells/mL) were bioprinted. In order to assess the cellular morphology and cartilaginous matrices generated by cells after 21 days of chondrogenic differentiation in constructs, scientists used histological staining. They revealed that the GelMA structures displayed a sparse cells distribution, although the cells had spherical morphology (Figure 3C(i, ii)). The silk fibroin/gelatin constructs showed a homogenous distribution of cells, and some of these cells exhibited a spread morphology on day 21 (Figure 3C(iii, iv)). The observed spread morphology could be owing to the adhesive sites in the silk fibroin/gelatin constructs[138].

3.2.2. GFs and signaling molecules

Promoting cellular proliferation, inducing cell differentiation, or enhancing tissue regeneration via incorporating GFs or other signaling molecules into bioinks is another topic worthy of discussion[139-141]. The desired cell/tissue-related properties of PBHs can be achieved by adding several GFs, such as insulin-like growth factor[142], vascular endothelial growth factor (VEGF)[143], stromal cell-derived factor-1α[144], fibroblast growth factor[145], and BMP-2[146], as well as signaling molecules, including exosomes, ECM granules, DNA, microRNA (miRNA), cytokines, bioceramics, and bioactive polymers, to name a few[147]. For instance, these biochemical factors are capable of improving cell differentiation by presenting cues that direct the differentiation of stem cells into specific cell types like bone or cartilage cells[148,149]. In this regard, a team of scholars[150] worked on the functional vasculature and osteogenesis of GelMA-based bioinks for application as large-scale bone tissue constructs. Within this novel study, GelMA bioinks (crosslinking approach: photo-crosslinking with 0.1% w/v Omnicure S2000 at 360–480 nm wavelength, UV light with 6.9 mW/cm^2, and exposure time of 20 s) functionalized/loaded with VEGF and silicate nanoplatelets that contained human umbilical vein endothelial cells (HUVECs) and hBMSCs (cell densities: 2×10^6 cells/mL) were bioprinted using extrusion-based printing. To construct a pattern with both capabilities of vascularization and osteogenesis, a HUVECs/hMSCs-encapsulated GelMA hydrogel (5% w/v) was bioprinted in the central area so that a blood vessel could be formed, and around this structure, they bioprinted silicate nanoplatelets-loaded, VEGF-functionalized GelMA hydrogel (10% w/v) embedded with hMSCs (cell density: 2×10^6 cells/mL) for inducing osteogenesis. It was revealed that a perfusable lumen possessing an endothelial lining at the construct's center was generated post-bioprinting. The hMSCs in the inner gel differentiated to the smooth muscle cells that could promote the formation, stabilization, and maturation

Tables 2. Summary of biophysical parameters affecting PBHs' bioprinting in the cartilage and bone TE

Considered factors	Bioink composition	Cell type (cell density)/ animal model/target tissue	Printing method/ crosslinking approach	Results	Reference
Composition	Alginate (0.8% and 1.8% w/v)/ gelatin (4.1% w/v)	P3 hMSCs (1.67×10^6, 5×10^6, and 15×10^6 cells/mL)/-/bone	Extrusion/physical crosslinking (ionic crosslinking)	• Higher content of DNA, enhanced expression of collagen type I–alpha-II, increased ALP activity, and stimulated osteogenic differentiation in soft scaffolds (0.8% w/v alginate) • Less mineralized tissue and lower mineral formation rate in stiff constructs • Observed cells with a 3D cellular network and osteoblast- and early osteocyte-related gene expressions in soft scaffolds	[114]
	GelMA (15% w/v)/HAMA (2% w/v) (1:1 and 2:1)	HuCol2gLuc (2×10^6 cells/mL)/-/cartilage	Extrusion/chemical crosslinking (photo-crosslinking)	• Enhanced chondrogenesis in the GelMA/HAMA bioink over the GelMA one alone • High cellular viability (≥ 90%) • Higher level of cellular mobility in the softer printed construct (1:1)	[115]
Biodegradation	GelMA (7% w/v)/GMHA (3% and 5% w/v)	Tonsil-derived MSCs (10×10^6 cells/mL)/female BALB/c nude mice/cartilage	Extrusion/chemical crosslinking (photo-crosslinking)	• Achieved a printed scaffold (7% GelMA/5% GMHA), being fairly stable, preserving its shape well, and having a low rate of degradation • High viability of cells and regenerated cartilage-like tissues • Enhanced expression of collagen type II and formed hyaline matrices 3 weeks post-implantation	[117]
	PEGDA (6% w/v)/gelatin (9% w/v)/SilMA (3% w/v)	Primary porcine chondrocytes (2×10^6 cells/mL)/-/cartilage	Extrusion/chemical crosslinking (photo-crosslinking)	• Delayed degradation rate after adding PEGDA to the composition • Obtained a printed hydrogel with 90% degradation after 28 days of incubation in protease enzyme	[118]
	SilMA (10%, 15%, and 25% w/v)	MC3T3-E1 preosteoblasts (2×10^6 cells/mL)/-/bone	DLP/chemical crosslinking (photo-crosslinking)	• Achieved degradation percentages of 91.0 ± 2.27%, 64.8 ± 3.2%, and 48.6 ± 2.15% at 21 days for groups of 10%, 15%, and 25% w/v SilMA scaffolds, respectively • Better proliferation and attachment of the cells in 15% SilMA construct	[119]

Porosity-related parameters	Collagen (1%, 3%, and 5% wt)	Rabbit articular chondrocytes (1×10^6 cells/mL)/female New Zealand White rabbits/cartilage	Extrusion/chemical crosslinking	• Observed mostly live cells in the porous constructs' cross-sectional live and dead image • Significantly improved *in vivo* regeneration of cartilage, and high levels of GAGs distribution in the porous scaffold-treated group • Observed severe irregularity in the articular surface and defect lesions in the non-porous scaffold-treated group	[121]
	GelMA (20% wt)/porogen (0.5%, 1.5%, and 3.0% wt)	hMSCs (2×10^6 cells/mL)/-/bone	DLP/chemical crosslinking (photo-crosslinking)	• Improved cell spreading in portions with larger pore sizes • Promoted cell cluster sizes in the gel regions containing 1.5% and 3.0% wt porogen • Enhanced cell proliferation in portions having higher porogen concentration, and increased expression of RUNX2 in the regions with larger pores and higher BMP-2 concentrations	[125]
Crosslinking process	Collagen (1%, 3%, and 5% wt)	Rabbit articular chondrocytes (1×10^6 cells/mL)/female New Zealand White rabbits/cartilage	Extrusion/chemical crosslinking (0.1, 1, and 5 mM of genipin)	• Higher compressive modulus for the construct crosslinked with a higher concentration of genipin and longer crosslinking time • Enhanced compressive modulus with the increment of crosslinking agent's concentration and crosslinking time • Achieved cellular survival > 90% at the crosslinking times of 0.5, 1, and 6 h at 0.1 mM genipin, gradually diminished cellular viability by the crosslinking time's extension from 0.5 to 6 h at 1 mM, and dramatically decreased cell survival at concentrations beyond 5 mM	[121]
	Collagen type I (5% wt)	MC3T3-E1 preosteoblasts (5×10^6 cells/mL)/-/bone	Extrusion/chemical crosslinking (0.1%, 0.25%, 0.5%, 1%, and 3% wt of TA)	• Enhanced stability and augmented mechanical strength in the TA concentration above 0.5% wt • Diminished degradation rate with the increase of TA concentration • Observed cell proliferation, enhanced DNA expression, and great survival of cells (approximately 95–96%) in all scaffolds	[133]

of vessels, as well as enhancing the HUVECs proliferation. Furthermore, HUVEC's survival and vasculogenesis were promoted possibly because of the VEGF that activated the VEGF receptors playing roles in the regulation of phosphoinositide 3-kinase (P13K) and focal adhesion kinase. They also reported that the encapsulated hMSCs formed a mature bone niche after 21 days of cultivation mainly due to the existence of silicate nanoplatelets, VEGF presence, and the osteogenic medium' sustained perfusion. Recently, a hBMSCs-loaded alginate sulfate/GelMA bioink (1% and 10% w/v) (cell density: 20×10^6 cells/mL) incorporating transforming growth factor beta-3 (TGF-β_3) was bioprinted employing extrusion printing technique (crosslinking approaches: photo-crosslinking with 0.05% w/v Irgacure 2959 at 365 nm wavelength, UV light with 5 mW/cm^2, and exposure time of 15 min, followed by ionic crosslinking with 50 mM $CaCl_2$ for 15 min) with the aim of articular cartilage repair. Sustained release of TGF-β_3 could provide an environment supporting robust *in vitro* chondrogenesis, with little evidence associated with the mineralization or hypertrophy over extended periods of culture. Moreover, *in vivo* 4-week results that included

the comparison of samples with and without GFs in a subcutaneously implantation BALB/c OlaHsd-Foxn1nu nude mice models showed that the groups treated with GF-loaded constructs had higher levels of sulfated GAGs (sGAGs) and collagen type II, as well as greater accumulation of matrix, indicating the formation of hyaline-like cartilage tissue[151]. Since exosomes act as media for communication between cells[152,153], a composite scaffold made up of decellularized cartilage ECM/GelMA (2% wt for ECM and 10% w/v for GelMA) containing BMSCs-derived exosomes bioinks was fabricated utilizing stereolithography 3D printing (crosslinking approach: photo-crosslinking with 0.25% w/v LAP at 405 nm wavelength, visible light, and exposure time of 30 s) for osteochondral repair by Chen *et al.*[139], and the therapeutic effects of MSCs-derived exosomes on osteoarthritis was examined using New Zealand White rabbit models. Interestingly, ECM/GelMA/exosome constructs could efficiently retain exosomes for at least 7 days, restore chondrocytes' mitochondrial dysfunction, improve cells migration, and polarize the synovial macrophage response toward an M2 phenotype. Comparing animals implanted with scaffolds with or without exosomes, it was demonstrated that ECM/GelMA/exosome-treated groups showed the formation of smooth tissues, regenerated fibrocartilage and hyaline-like cartilage, and more ossified tissues at 6 weeks post-implantation. The International Cartilage Repair Society (ICRS) scoring indicated a higher score for animals treated with exosome-embedded structures (14.1 ± 0.71) than the ECM/GelMA-and GelMA-treated groups (12.2 ± 0.61 and 7.8 ± 0.39, respectively) at 6 weeks after implantation. Each tissue's ECM generates a very unique tissue-specific microenvironment for the resident cells, which can provide them with the biochemical signals required for their functioning. Within an innovative evaluation, Isaeva *et al.*[154] assessed two compositions of collagen-based bioinks (4% w/v for pig atelocollagen type I) printed via extrusion printing: (i) with hMSCs (isolated from human adipose tissue) and (ii) with decellularized ECM granules (2.5% w/v with a particle size of 280 μm) and hMSCs (cell density: 5×10^6 cells/mL) for cartilage TE. After bioprinted constructs' subcutaneous implantation in white male rats, two groups were compared from various perspectives. In the first group (MSCs only), scholars observed the formation of a connective tissue capsule with multiple blood vessels and detected cells with cytoplasm including collagen type II 2 weeks post-implantation. The only evidence of the formed cartilage was the small islands of cartilaginous tissue with irregular shapes adjacent to the construct (Figure 3D(i–iv)). In the second group (decellularized ECM granules + MSCs), generation of a cartilage tissue was shown 2 weeks after implantation. Interestingly, chondroblasts could form tiny isogenic groups with an ECM having a pronounced perichondrium, and the produced ECM accumulated a great content of GAG. Moreover, an intense reaction to collagen type II by the tissue and signs of reduced proliferative activity were found (Figure 3D(v–viii)).

3.2.3. Cell signaling

The behaviors of cells within the bioprinted constructs are influenced not only by the bioinks cues but also by the signals from other cells as well as various types of intercellular signals, including autocrine, intracrine, endocrine, paracrine, and juxtacrine signals, categorized based on the distance between responder cells and signaling. Of note, paracrine and juxtacrine signaling pathways are of higher significance in bioprinting of stem cells owing to the size of printed structures. In juxtacrine signaling and via molecule transfer through gap junction channels that are along the surface of contact, intercellular communication is realized[155]. Stem cells, tending to form aggregates, are deeply affected by cluster situation under the mentioned mechanism. Specifically, the degree of MSCs differentiation into osteogenic lineage is revealed much greater in aggregated cells compared with isolated ones[46]. Furthermore, the stem cell aggregates' size is capable of regulating the differentiation fate[156]. By controlling the bioprinting volume, initial seeding density of cells, and cultivation time, stem cell aggregates with regular shapes and uniform sizes can be created through cellular proliferation post-bioprinting[157]. Signaling cells release paracrine signals, and they target the nearby cells. In this regard, one of the most essential uses is the co-culture of several cells in order to enhance cellular functions[9,69], and another approach to control the migration of cells is the co-printing of different cell types[158]. Additionally, multiple cells' deposition in arranged positions facilitates the complex tissues' construction, and regulation of cellular survival and density can influence the bioactive proteins' local concentration, further affecting the stem cell differentiation[159]. Table 3 recapitulates the biochemical parameters influencing PBHs' bioprinting in the cartilage and bone TE.

In a nutshell, the behaviors of cells encapsulated in the PBHs are affected by biophysical cues, including composition, biodegradation, porosity-related parameters, and crosslinking process. In this regard, elastic stiffness, degradation rate, pore size, porogen concentration, as well as time and concentration of the used crosslinker, which exert various effects on cell viability, proliferation, differentiation, and tissue regeneration, should be considered and optimized with respect to the PBHs. Furthermore, biochemical cues, such as chemical

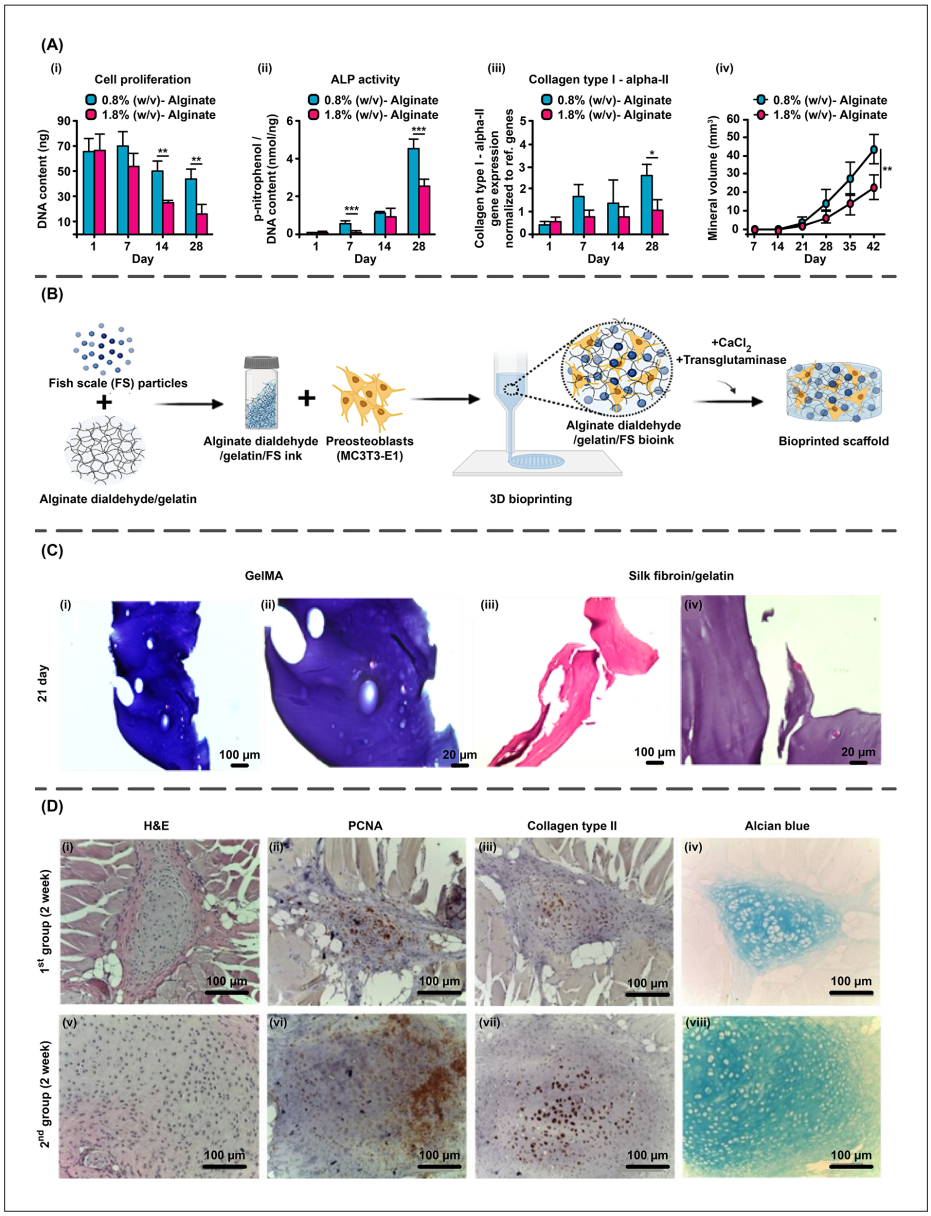

Figure 3. (A) (i) The content of deoxyribonucleic acid (DNA), (ii) alkaline phosphatase (ALP) activity, and (iii) gene expression of collagen type I–alpha-II associated with the printed constructs after cultivation in the osteogenic media at days 1, 7, 14, and 28. (iv) Mineral volume related to the bioprinted scaffolds from days 7 to 42 ($^{*}p < 0.05$, $^{**}p < 0.01$, and $^{***}p < 0.005$). Reproduced under the terms of the Creative Commons Attribution 4.0 International (CC BY 4.0) license[114]. Copyright 2020, Elsevier. (B) The schematic presentation of the cross-linked alginate dialdehyde/gelatin/FS particles bioprinted scaffold including preosteoblast MC3T3-E1 cells. Reproduced under the terms of the Creative Commons Attribution 4.0 International (CC BY 4.0) license[137]. Copyright 2023, IOP Publishing Ltd. (C) The hematoxylin and eosin (H&E) images of the (i, ii) GelMA and (iii, iv) silk fibroin/gelatin bioprinted constructs on day 21 (scale bars: 100 and 20 µm). Reproduced under the terms of the Creative Commons Attribution 4.0 International (CC BY 4.0) license[138]. Copyright 2023, IOP Publishing Ltd. (D) The cartilage tissue in rat models of two experimental groups (objective lens × 20 and scale bar: 100 µm). (i–iv) The first group (MSCs only), 2 weeks. (v–viii) The second group (decellularized ECM granules + MSCs), 2 weeks. (i, v) H&E staining; (ii, vi) proliferating cell nuclear antigen (PCNA) staining; (iii, vii) immunohistochemical staining for collagen type II; (iv, viii) Alcian blue staining. Reproduced under the terms of the Creative Commons Attribution 4.0 International (CC BY 4.0) license[154]. Copyright 2022, MDPI.

structure, presence of GFs and signaling molecules, as well as cell signaling impact cell properties like cellular survival, adhesion, differentiation, and ECM formation, to name a few. To achieve the best cell-related results, scholars must pay meticulous attention to the RGD or MMP sequences proteins possess, GFs or other signaling molecules (exosomes, DNA, miRNA, cytokines, bioceramics, and bioactive polymers) that can be introduced based on the

specific tissue (cartilage or bone), and different signaling pathways which occur within the cells (autocrine, intracrine, endocrine, paracrine, and juxtacrine signaling) or those received from other cells. In the fields of cartilage and bone TE, several research projects have been conducted so far to assess the impacts of mentioned environmental cues on the cellular features and tissue development ability of the PBHs. The original experiments mentioned above, alongside the achieved outcomes, will hopefully provide a comprehensive roadmap to move these fields forward.

4. Process compatibility considerations of PBHs

Bioprinting requires the proper design of a bioink to support tissue growth, cellular viability, and printability[160], and an efficient transfer of nutrients and oxygen within the bioink must be ensured by the PBH's structure[161].

Biocompatibility and mechano-rheological features are primarily responsible for bioink printability. Biocompatibility is essential in developing bioinks to prevent adverse effects on the viability, proliferation, or differentiation of cells encapsulated within[162]. Moreover, a bioink with appropriate mechano-rheological characteristics can be extruded easily, maintain its shape after printing, and support the deposition and organization of encapsulated cells into a desired structure. Although many PBHs, such as collagen and fibrin, exhibit the above-mentioned qualities, they cannot be readily tailored, and there are several challenges in their printing[163]. Bioprinting strategies and bioink properties are directly influenced by chemical, physical, and biological characteristics; in this regard, Figure 4 presents key considerations required for bioprinting cell-laden PBHs.

4.1. Mechano-rheological considerations

To be an optimal bioink for various bioprinting modalities, a material must possess several essential characteristics; for instance, a major factor affecting biomaterial printability is its mechanical properties. In multiple cases, scholars perform long-term incubation of cell-laden constructs for tissue development, and an integral part of this procedure is guaranteeing structural integrity. Notably, a printed construct should provide oxygen and nutrient transport into the cells, a critical subject to consider when designing its architecture[164].

Inkjet and extrusion-based bioprinting techniques are based on viscoelasticity and rheological characterization. PBHs and the amino acid sequences of fibrous proteins, including collagen, elastin, silk fibroin, keratin, resilin, and fibrin, play both mechanical and architectural roles in nature, which make them attractive choices for these

Tables 3. Recapitulation of biochemical parameters affecting PBHs' bioprinting in the cartilage and bone TE

Considered factors	Bioink composition	Cell type (cell density)/ animal model/target tissue	Printing method/ crosslinking approach	Results	Reference
Chemical structure	Gelatin (1.5% w/v)/ silk fibroin (7% w/v)	Primary chondrocytes (10^6 cells/mL)/-/ cartilage	Extrusion/physical crosslinking	• Enhanced cellular viability, improved cell adhesion, and increased ECM formation compared to controlled group • Improved printability due to the shear-thinning behavior of silk and the high viscosity of gelatin	[136]
	Sodium alginate dialdehyde (7.5% w/v)/ gelatin (15% w/v) with FS particles	Mouse MC3T3-E1 preosteoblasts (5×10^6 cells/mL)/-/bone	Extrusion/physical and chemical crosslinking (ionic and enzymatic crosslinking, respectively)	• Promoted cellular proliferation during 28 days of cultivation	[137]
	GelMA (10% w/v) and silk fibroin/ gelatin (80 mg of gelatin powder in 800 µL of silk fibroin solution)	hBMSCs (1×10^7 cells/mL)/-/cartilage	Extrusion/chemical crosslinking (photo-crosslinking and enzymatic crosslinking)	• Observed sparse distribution of cells with spherical morphology in GelMA structures • Homogenous distribution of cells with some of them exhibiting a spread morphology on day 21 in silk fibroin/gelatin constructs	[138]

	GelMA (15% w/v)/ VEGF/silicate nanoplatelets	HUVECs and hBMSCs (2×10^6 cells/mL)/-/bone	Extrusion/chemical crosslinking (photo-crosslinking)	• Generated perfusable lumen possessing an endothelial lining at the construct's center post-bioprinting • Differentiation of hBMSCs in the inner gel to the smooth muscle cells, promoting the formation of vessels and enhancing the HUVECs proliferation • Promoted HUVEC's survival and vasculogenesis, as well as formed mature bone niche by hBMSCs after 21 days	[150]
	Alginate sulfate (1% w/v)/GelMA (10% w/v)/ TGF-β_3	hBMSCs (20×10^6 cells/mL)/BALB/c OlaHsd-Foxn1nu nude mice/cartilage	Extrusion/chemical crosslinking (photo-crosslinking)	• Supported robust *in vitro* chondrogenesis due to the sustained release of TGF-β_3, with little mineralization or hypertrophy • Higher levels of sGAGs and collagen type II, as well as greater accumulation of matrix in groups treated with GF-loaded constructs	[151]
	Decellularized cartilage ECM (2% wt)/GelMA (10% w/v) containing BMSCs-derived exosomes	-/New Zealand White rabbits/osteochondral	Stereolithography/ chemical crosslinking (photo-crosslinking)	• Achieved constructs retaining exosomes, restoring chondrocytes' mitochondrial dysfunction, improving cells migration, and polarizing the synovial macrophage response towards an M2 phenotype • Formation of smooth tissues, regenerated fibrocartilage and hyaline-like cartilage, and more ossified tissues in ECM/GelMA/ exosome-treated groups • Higher score for animals treated with exosome-embedded structures at 6 weeks after implantation	[139]
GFs and signaling molecules	Atelocollagen type I (4% w/v) with (i) hMSCs and with (ii) decellularized ECM granules (2.5% w/v) and hMSCs	hMSCs (5×10^6 cells/mL) white male rats (155–230 g; aged 1.5–2 months)/cartilage	Extrusion/-	• Formation of a connective tissue capsule with multiple blood vessels and detected cells with cytoplasm including collagen type II in the first group • Small islands of cartilaginous tissue with irregular shapes adjacent to the construct in the first group • Generation of a cartilage tissue with chondroblasts forming tiny isogenic groups, and the produced ECM having a great content of GAG in the second group • Observed intense reaction to collagen type II by the tissue and signs of reduced proliferative activity in the second group	[154]

bioprinting techniques[165,166]. It needs to be considered that by extraction and purification procedures, proteins can be degraded which negatively impacts their molecular weight, an essential parameter influencing rheological properties[167]. To achieve the required purification degree while ensuring the best quality, selecting the proper

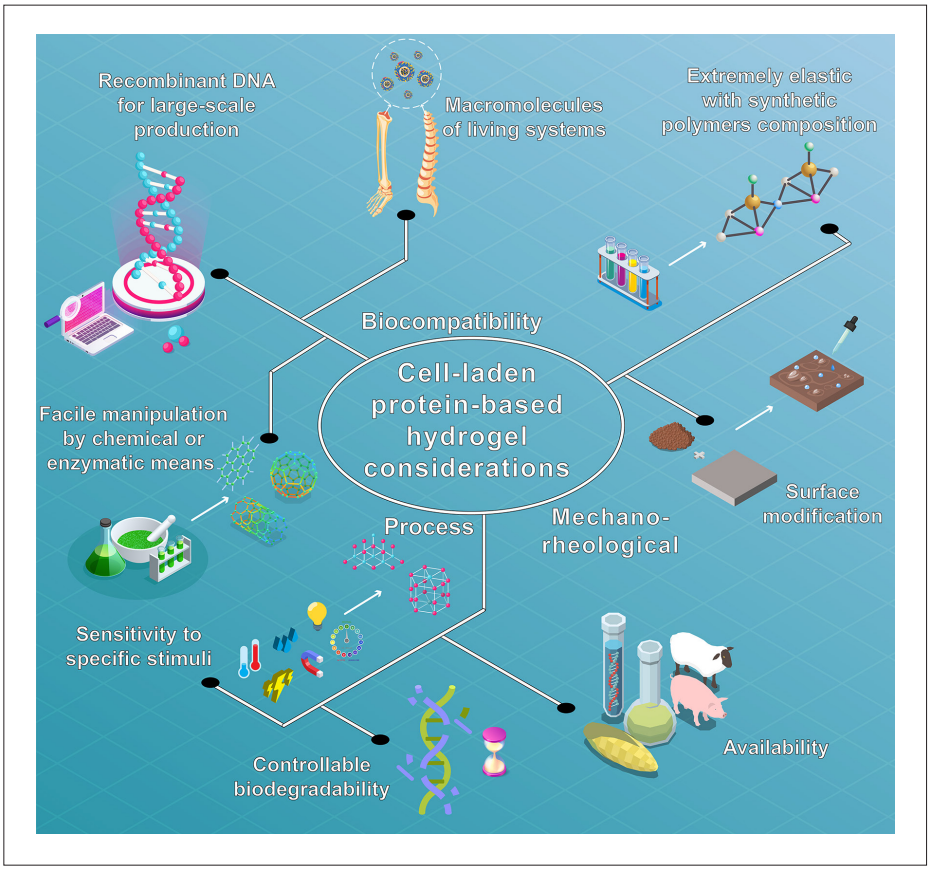

Figure 4. Bioink considerations needed to obtain cell-laden protein-based hydrogel (PBH) construct.

extraction method is of great importance when a PBH is developed. The characteristics of protein-based materials are significantly affected by the extraction technique and the utilized raw material, mainly due to the structure, molar mass distribution, composition, and functional properties of these materials[168]. Of note, protein molecules are entangled above a critical molecular weight, resulting in a proportional relationship between viscosity and molecular weight[168].

The presence and density of cells impact the rheological and mechanical features of inks. As a result of incorporating cells into a cell-barren gel-phase bioink, as well as increased cellular density, decreased degree of crosslinking, liquid viscosity, and final mechanical properties were observed[169]. Following this, rheological characteristics of the bioinks affect cellular viability during bioprinting; therefore, shear-thinning bioinks are more desirable because they shield cells and enable high-resolution printing simultaneously. Indeed, hydrogels should protect cells from exerted shear forces when the bioink is printed through the bioprinters' nozzles. After gelation, cell-laden hydrogels must have a storage modulus greater than the loss modulus in order to maintain their shape, indicating more viscoelastic behavior and thus greater printability. High protein concentration aids in minimizing post-printing shrinkage caused by ambient conditions; hence, better integrated mechanical properties are obtained[169-172]. Although augmenting the bioink's concentration via enhancing the viscosity reduces the distortion, increasing the concentration of PBHs diminishes the micro-roughness of the bioprinted scaffolds[25].

In the bioprinting fabrication method, viscosity describes the resistance of a bioink to deformation. Extruding bioinks with high viscosities and maintaining their shape post-printing are possible; however, encapsulated cells can be afflicted during the extrusion process because the deforming forces are high[173]. Another problem is associated with the release of shear forces after printing, which raise viscosity and inhibit the flow of printed constructs. On the other hand, the lower viscosity of bioinks leads to less nozzle clogging and allows the mixing of cells, but it can also result in poor feature definition since the bioinks cannot retain their shape subsequent to

the extrusion. Notably, a bioink's viscosity relies on factors like temperature, concentration, molecular interactions, and molecular weight[174].

Owing to the interactions that occur between hydrophobic domains within the sequence of proteins, shear forces moderately transform the liquid into solid structures (random coils to β-sheets) during the extrusion process. Unfortunately, degradation occurs in the production of proteins, affecting their rheological properties and printing. Besides, bioprinting lacks the solution's flow-induced extensional stretching, which diminishes the hydrogel viscosity and makes maintaining a stable structure difficult[175-177].

Before printing, the distribution of velocity and shear stress across the cross-section of a nozzle is zero. Additionally, a dispensing process cannot be carried out without shear stress[173]. In fact, hydrogels are subjected to shear stresses, at the nozzle walls in particular, at the time of printing. A number of parameters determine the amount of shear stress exerted on the bioink and embedded cells, such as printing pressure, nozzle diameter, and bioink viscosity[178]. In general terms, cells exposed to low shear forces tend to survive longer; conversely, high shear stresses can decrease cellular viability[179].

The shear stress generated in bioprinting does not pose an obstacle for small, globular proteins, but in the case of their larger, more fragile counterparts, structural integrity can be threatened[180]. As Nishioka *et al.*[181] argued higher compression rates that were employed to create droplets resulted in more protein denaturation and biological inactivity, and without the use of stabilizing additives, the enzyme activity was reduced under all printing conditions. It could have been possible to mitigate the adverse effects of bioprinting if sugars like trehalose and glucose were added to help preserve the enzymatic activity. This outcome raises some interesting queries regarding how proteins are denatured on the nanoscale as a corollary to maintain their bioactivity while growing crystals. It is worthy to mention that a protein's native secondary structure may be primarily determined by its amino acid sequence if the protein is small and globular; however, if the protein has deeply folded pockets functioning as catalytic sites, such as most of the active enzymes, then this rule may not always hold true[182].

By the same token, when printing biomaterials, yield stress specifies the force required in order to permit smooth, continuous extrusion[87,183] and ensures the homogeneity of encapsulated cells within bioinks. In the absence of forces, hydrogels with low yield stress leak out of nozzles or experience phase separation[184,185]. Of note, bioinks with high viscosities may maintain their shape for a short period of time in a bioprinted structure, but those with high yield strengths can hold shapes much longer. The yield stress is generated as a result of the viscosity peak, and when viscosity is plotted against shear stress, yield stress can be determined as the threshold value beyond which the material begins to flow[186]. Shape-retaining structures are typically produced by inks with high yield stresses; accordingly, adding bulking agents and thickeners, such as gellan, improves the PBHs' yield stress[187]. Moreover, high yield stresses can negatively influence cells when bioinks initiate flow[188]. Another subject is that hydrogels with cell-laden networks should be able to self-recover following printing because their physical crosslinking network is broken by the shear stress[189]. For the rapid recovery of the hydrogel's viscosity after applying a shear rate, a sharp decrease in the viscosity when the shear rate is applied is indeed ideal[190]. In addition to being mechanically strong, the extruded hydrogel filament must be capable of maintaining its shape subsequent to printing, as mentioned previously; thus, thixotropic properties are essential factors when evaluating a hydrogel's suitability for bioprinting[164].

From another viewpoint, for achieving optimum features of cell-laden printed structures, such as obtaining a filament diameter that matches the diameter of the nozzle, strand uniformity, and accurate strand placement, printing parameters like pressure and dispensing speed are often varied; nevertheless, these factors can influence the viability of extruded cells[191]. According to the scholars' investigation, increasing the applied pressure reduced the survival of encapsulated cells, regardless of whether the bioinks were liquid or gel[192]. The nozzle's diameter and shape should also be considered; within this context, a study by Billiet *et al.*[193] reported that cells in gel-phase bioinks were more viable when loading bioinks in conical nozzles compared with cylindrical ones. Furthermore, the shear stress increases with the increment of nozzle length, so analyzing varying nozzle lengths is of crucial significance for drawing firm conclusions between using tapered conical nozzles and cylindrical ones. Cell viability is also decreased when the nozzle diameter is reduced in cylindrical nozzles; to be more specific, the majority of cells are under highly stressful conditions, meaning that high pressure and a small diameter can cause necrosis rather than apoptosis, and the nucleus experiences morphological and irreversible damage[194].

In addition, strand stretching and thinning can result from bioprinting with a high speed at a given pressure[195]. The polymer matrix probably introduces potentially undesirable tensile and compressive forces to the cells, assisting with cell alignment along the bioprinted strand. Depending on the cells' location within a filament, cell survival and morphology may differ[196]. For instance, in the

case of nozzle walls, there may be an increase in shear stress at the strand's periphery, leading to lowered cellular viability. It is likely that the peripheral filaments tend to spread and form cellular networks more quickly because they are in the vicinity of the hydrogel surface and are not encapsulated completely[197]. A functional difference between two cells may also be the result of morphological differences between their filaments on the exterior and the interior. When this matter is viewed from the perspective of bioprinting approaches, for example, in an acoustic bioprinter, a pool of bioink is directly injected with cell-encapsulated droplets and deposited over the surface[67]. Due to its nozzle-free design, this technology avoids clogging issues and prevents detrimental shear stresses, heat, and pressure commonly experienced in other bioprinting methods[198,199].

The bioprinting of embedded cells has previously been done employing inkjet and extrusion technologies[200,201]. For maintaining cell viability, a PBHs was used to suspend cells in the inkjet fluid reservoirs utilized for bubble-jet technology or closed fluid reservoirs utilized for piezoelectric technologies in order to buffer them from temperatures between 200 and 300°C[202]. Additionally, inkjet and extrusion technologies subject cells and protein structures to remarkable mechanical and thermal stresses. Exhibiting poor directionality of droplets or continuous filaments, achieving non-uniform droplet sizes, existing mechanical shear stress of ejected cellular materials at the nozzle, and having routine nozzle clogging problems are other drawbacks of these techniques; as a result of the mentioned obstacles, large numbers of "empty" droplets are generated, contributing to significant inefficiency[66].

Although the nozzle geometry has no impact on the droplet size or ejection directionality, it has been demonstrated that the geometry can cause damage to cells or denature protein structures in printing methods like inkjet and extrusion. Since acoustic bioprinting employs very short durations and low wavelengths, its effects on cell membranes and protein structures are negligible. It is also noteworthy to mention that during ejection, no high pressure or heat is applied to the fluid[66,203].

Therefore, optimizing the PBHs' concentration to obtain optimal viscoelasticity properties during bioprinting is necessary. Concerning this matter, the investigation conducted by Singh *et al.*[136] focused on the development of silk-gelatin bioinks for the cartilage tissue's microextrusion bioprinting. In the first step, silk (0.5% to 2% w/v) and gelatin (1% to 9% w/v) hydrogels loaded with porcine auricular chondrocytes (1×10^6 cells/mL) were prepared. Afterward, the viscosity and modulus were evaluated in the range of 4–45°C so as to obtain a viscoelastic range for their bioink. They illustrated that the combination of the shear-thinning rheological behavior of silk due to β-sheet crystallization and gelatin's high viscosity enhanced the bioink's printability, and the bioink viscosity value was the lowest in the range of 25–35°C, enabling printing within this temperature range. Furthermore, high cellular survival was ensured when gelatin and silk concentrations were 7% and 1.5% w/v, respectively.

Since compressive and tensile behaviors of the bioprinted hydrogels are critical, Yang *et al.*[204] used collagen (15 mg/mL) and alginate (15 mg/mL) mixed with new-born Sprague Dawley chondrocytes (10×10^6 cells/mL) as a bioink to print 3D six-layer constructs (2×2 cm^2) and assessed their mechanical features. Uniaxial tension tests were conducted at ambient temperature with constructs stretched at 2 mm/min. Besides, cell-laden gels with a maximum displacement of 1 mm and a speed of 0.1 mm/min were analyzed for their compressive strength. Compared with the alginate alone (~28 kPa), collagen increased the stiffness of collagen/alginate-printed hydrogel by nearly 1.87 times. Additionally, the printed composite hydrogel (~41 kPa) showed remarkable strengthening and toughening effects with 162.08% greater strength and toughness than the alginate gel (~19 kPa).

4.2. Biocompatibility considerations

Biocompatibility refers to the material's ability to respond to a specific host environment[205]; within this context, it is essential to consider the biocompatibility of cell-laden PBHs during bioprinting, *in vitro* maturation, immunogenicity of hydrogels, and long-term effects of the gels.

Cellular viability and proliferation can be influenced by the hydrogel composition once bioinks have been deposited. In numerous matrix proteins and as mentioned, the RGD motif improves the cell–matrix interactions and can promote osteogenic differentiation and cell survival. It is also possible to modify hydrogels with other side groups and sequences like phosphate groups, covalently bound GFs, and heparin-binding domains, with the aim of increasing the creation of mineralized matrices and bone tissue possessing comparable mechanical features[206,207]. Compared with synthetic polymers, protein-based polymers like collagen, silk, keratin, serum albumin, and elastin have cell-adhesive peptide sequences that provide conducive microenvironments suitable for enhancing cell survival and proliferation[208]. In addition, physiological and biological cues present in structural proteins play a crucial role in bioink development. Additionally, protein-based materials are not only environmental friendly and renewable but also strong, elongated, tough, and slowly degradable. As an example, silk fibroin is one of the most popular PBHs used in bioprinting. It undergoes a remarkable structural transition from a random-coil to a

β-sheet structure, and aqueous silk fibroin solution contains hydrophobic domains that self-assemble into 3D hydrogels. As an amphiphilic material, it is capable of entrapping water and forming bioinks suitable for preventing cell dehydration in bioprinting. Thus, these kinds of PBHs are ideal bioinks for the bioprinting process since they are biocompatible, tunable, biodegradable, and capable of self-assembly[209,210]. It is also important to note that spidroins 1 and 2 are two major ampullates (draglines) in silk with a highly repetitious amino acids' core sequence, conjugated to the non-repetitive N-and C-terminal domains on either side, resulting in a bulging protein structure. By virtue of this property, hydrophilic domains are enclosed within the micelles, whereas hydrophobic terminal domains build the edges, ensuring that proteins are stable. This feature is essential for creating precise cell-laden PBHs that can be bioprinted employing this technology[211,212].

Regarding the impact of bioink concentration on cell viability, high concentrations can cause more pressure on the printing nozzle, followed by the generation of high level of shear stresses that are damaging to cells. As a result, the survival of cells should be evaluated at various levels of bioink concentration to enhance the cellular performance[213]. In order to induce solidification by sol-to-gel transition, factors like pH changes, temperature, and crosslinking approaches may rupture cell membranes, cause apoptosis and necrosis, or denature biological components (e.g., GFs and proteins) that are mixed with the bioink for developing biomimetic tissues[214-216].

High cell viability during bioprinting and maintenance of cellular survival for extended periods are of high priority[217]. As the printing process progresses, numerous external factors influence the viability of cells, such as printing modules and materials concentrations. Besides, the bioprinting process exerts mechanical forces on cells, causing deformation and breaching their membranes. Despite of cells' ability to resist specific force levels, their integrity can be lost if subjected to excessive stresses[218]. Therefore, recognizing the cell damage mechanisms during the bioprinting process to maintain cell viability, one of the basic requirements of bioprinting, is critical. Cell viability can also be affected by thermal and shear stresses that create cell-laden PBH drops. Scientists have reported that cells under local temperatures of up to 300°C are not greatly harmed via short exposures of 2 μm during the printing process[219,220]; in contrast, the vibrations and wave frequencies of piezoelectric bioprinting can disrupt cell membranes as well as unfold protein structures[221]. Moreover, in laser-assisted bioprinting, the encapsulated living cells and/or proteins are coated with hydrogel beforehand, and the absorption layer is transparent to the laser light; these phenomena inflict less damage to the protein structure and cell membrane, which improves cell survival[222].

Rhee *et al.*[106] focused on high-density cell-laden PBHs. In this regard, primary fibrochondrocytes from bovine joints (10×10^6 cells/mL) were mixed with the collagen hydrogel, and the bioprinted constructs were then tested for cell viability and mechanical properties. Accordingly, cells within the constructs were generally 90% viable immediately after printing. In addition, neither the cell numbers nor their viability varied with time over 10 days. A compressive modulus of 30 kPa was achieved at the highest printing concentration of collagen hydrogel (17.5 mg/mL). Therefore, their constructs demonstrated excellent mechanical stability and could support and maintain cell growth. In another pioneering investigation, silk-glycidyl methacrylate (Silk-GMA) loaded with human chondrocytes was fabricated by Hong *et al.*[223] for producing engineered cartilage with functional and efficient features. They bioprinted hydrogels ($5 \times 5 \times 2$ mm^3) containing human chondrocytes (1×10^6 cells/mL) and NIH 3T3 fibroblast cells combined with the Silk-GMA bioink. Likewise, 30% Silk-GMA solution comprising human chondrocytes (10×10^6 cells/mL) was bioprinted in the shape of a trachea ring (external diameter: 7 mm, internal diameter: 5 mm, and height: 2 mm) for *in vitro* cartilage TE. Within a novel research, Ren *et al.*[91] used an extrusion-based bioprinter to fabricate collagen type II hydrogel constructs embedding chondrocytes from New Zealand White rabbits' knee joints. Three groups were created based on the density of total cells incorporated into the collagen type II pre-gel (20×10^6, 10×10^6, and 5×10^6 cells/mL). The constructs were crosslinked for 30 min at 37°C in a humidified incubator and were cultured at 0, 1, 2, and 3 weeks. Interestingly, 98 ± 1% of chondrocytes were alive. Viability tests were conducted on the first day following synthesis in order to evaluate the damage caused by bioprinting to cells; 93 ± 3% of living cells were present in varying groups with no significant difference between them (Figure 5A). Based on the results, bioprinted hydrogel constructs with biomimetic cell density gradients can be utilized to fabricate engineered cartilage tissues.

The experiment, explained earlier, on engineering P3 hMSCs-encapsulated alginate/gelatin bioinks (4.1% w/v for gelatin and 0.8% w/v for alginate) (cell density: 1.67×10^6, 5×10^6, and 15×10^6 cells/mL) for bone TE illustrated that after 21 days of culture, the cells could spread and form a 3D interconnecting network in all groups, particularly in the 15×10^6 cells/mL bioink (Figure 5B)[114]. The above-mentioned investigation on developing arch-like bioprinted structures using GelMA and silk fibroin/gelatin

bioinks loaded with hBMSCs (cell density: 1×10^7 cells/mL) for cartilage TE reported that the silk fibroin/gelatin construct contained more viable cells compared with the GelMA-printed structure (Figure 5C(i, ii)). Moreover, a significant difference in the survival percentage was seen ($p < 0.0001$) between the silk fibroin/gelatin constructs (91.16%) and the GelMA constructs (89.25%) after 14 days of culture (Figure 5C(iii))[138]. Additionally, the scholars that designed mouse preosteoblast MC3T3-E1 cells-loaded sodium alginate dialdehyde/gelatin bioinks containing FS particles (1%, 3%, 5%, and 10% w/v) (cell density: 5×10^6 cells/mL) for bone regeneration also assessed the cytocompatibility, and it was demonstrated that cells were

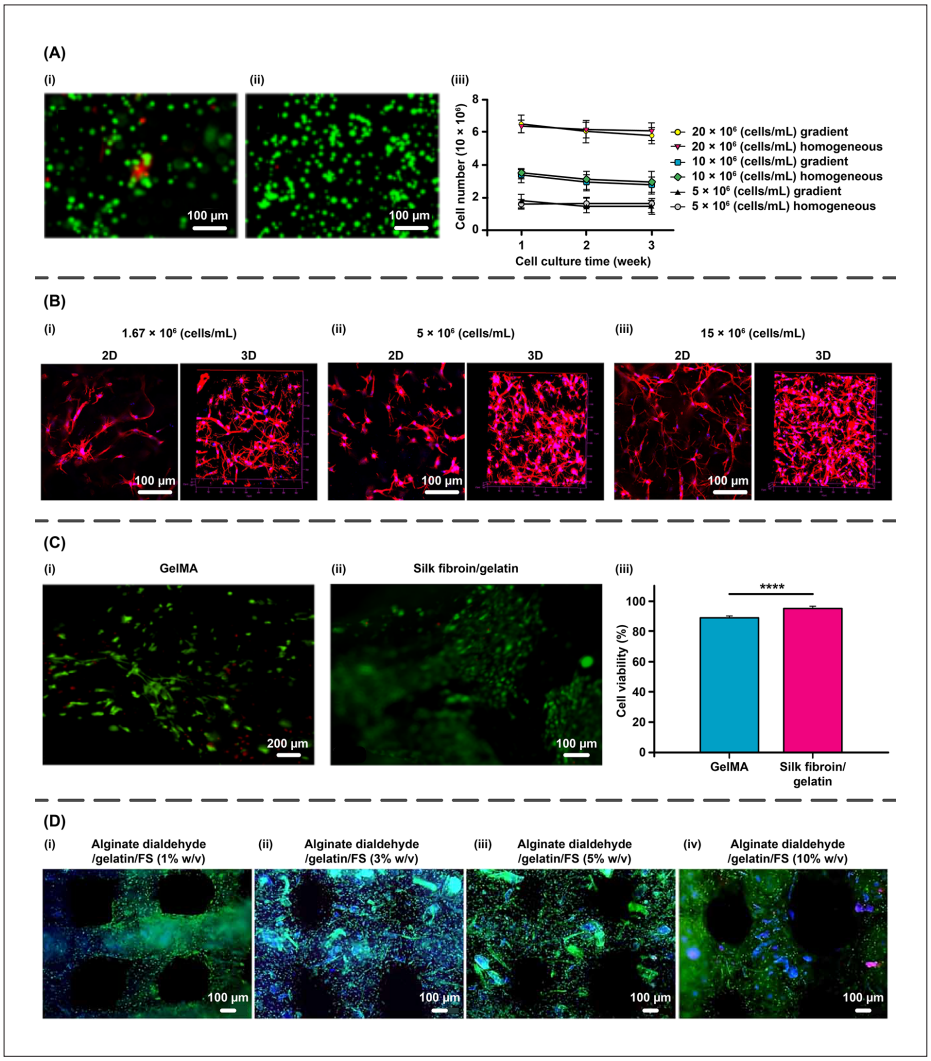

Figure 5. (A) The depiction of cell survival in the constructs and the total number of cells. The images (i) and (ii) illustrate the construct's middle zone after 2 weeks of *in vitro* cultivation and its superficial zone after 3 weeks of culture. Of note, calcein acetoxymethyl ester staining was done on live cells (green dots), and propidium iodide staining was performed on dead cells (red dots) (scale bars: 100 μm). (iii) The total number of cells within the structures after *in vitro* culture for 3 weeks in three groups. Reproduced under the terms of the Creative Commons Attribution 4.0 International (CC BY 4.0) license[91]. Copyright 2016, Springer Nature. (B) The bioprinted cell-laden structures' 2D and 3D actin staining images with various cell densities after 21 days of culture. Reproduced under the terms of the Creative Commons Attribution 4.0 International (CC BY 4.0) license[114]. Copyright 2020, Elsevier. (C) Live/dead assay of the bioprinted (i) GelMA construct and (ii) silk fibroin/gelatin structure after 14 days of culture. Live cells are shown in green (calcein acetoxymethyl ester) and dead cells in red (ethidium homodimer). (iii) The graph displaying the cell viability of hBMSCs on day 14 for the bioprinted constructs ($^{****}p < 0.0001$). Reproduced under the terms of the Creative Commons Attribution 4.0 International (CC BY 4.0) license[138]. Copyright 2023, IOP Publishing Ltd. (D) Live/dead assays of cells within and on the surface of the printed gels subsequent to 14 days of incubation (scale bars: 100 μm). The staining with 4',6-diamidino-2-phenylindole (DAPI) (blue), propidium iodide (red), and calcein AM (green) visualizes cell nuclei, dead cells, and viable cells, respectively. Reproduced under the terms of the Creative Commons Attribution 4.0 International (CC BY 4.0) license[137]. Copyright 2023, IOP Publishing Ltd.

viable and preserved their survival within various bioink compositions after 14 days of cultivation (Figure 5D)[137].

4.3. Crosslinking considerations

A bioprinted construct's degradation rate can be impacted by its composition, concentration, temperature, mechanical force, and cell culture medium; thus, the degradation rate of the bioprinted structure should be considered[164]. Specifically, the degradation rate of the PBHs is highly dependent on the β-sheet crystals' orientation, content, and non-crystalline domains[210,224]. The mechanical properties of bioinks may decrease too rapidly during culturing. To further enhance the integrity of the printed structures, crosslinking is most commonly performed for the printing of the dispensed cell-laden PBHs as stated[225]. It was mentioned that there are several kinds of crosslinking approaches used in PBHs bioprinting, including physical, chemical, and enzymatic crosslinking before, during, and after printing. Furthermore, thermal crosslinking can be used to print PBHs; in this case, temperature-induced gelation improves the printed construct's initial stability since it is faster than the gelation by Ca^{2+} cations as physical crosslinkers. Nevertheless, it is challenging to precisely control how much crosslinking occurs, and overheating in this process may adversely affect cell viability. Natural hydrogels, such as collagen, will lose mechanical strength because of enzymatic hydrolysis, and thermally sensitive hydrogels can also lose their shape when the environment's temperature changes[120]. For instance, due to the collagen helices' collapse to random coil structures at 30–35°C, the dissolved collagen's storage modulus and viscosity are rapidly reduced without gelation; hence, the thermal sensitivity of PBHs should be noticed in the bioprinting process[121,211]. Owing to this subject, scholars should meticulously select hydrogels and their associated 3D structures in a way that the degradation rate will be appropriate. One of the most common approaches in bioink printing is the employment of UV crosslinking to augment mechanical characteristics and degradation after bioprinting[169]. Nonetheless, variations in the UV exposure times decrease cell viability by increasing crosslinking after bioprinting[226]. Post-printing crosslinking can provide hydrogels with a higher modulus, as well as longer rates of degradation *in vitro* and *in vivo*, together with providing cells with proper stiffness[218,227]. Within a brand-new assessment, bioprinting of methylcellulose (MC)/GelMA bioinks with great shape integrity was performed. This research project introduced a new type of MC/GelMA bioink that could maintain its shape integrity over several months in the biological media. Unlike pure MC inks, distorting and dissociating in the biological media, MC/GelMA bioinks maintained their stability because of the GelMA's permanent photo-crosslinking under UV irradiation for 60 s. The results indicated that the swelling ratio was strongly influenced by the crosslinking density of the 3D network; a higher crosslinking density caused segments between joint points to become smaller, thereby preventing swelling. As a result of the photo-crosslinking of GelMA polymer chains, a covalent crosslinking network formed, which prevented the hydrogel from dissolving. The slow degradation of MC/GelMA hydrogel ensured that it retained its mechanical properties so that newly formed tissues and cells could be supported during regeneration. The MC/GelMA bioink's shape integrity was characterized by its complex modulus and yield stress, which were higher than those of the pure MC ink, resulting in self-supporting behavior once printed. Additionally, human primary osteoblasts that were encapsulated within the MC/GelMA hydrogels illustrated a cell survival of over 95%. This work emphasizes the importance of rheological features and the post-crosslinking process in the production of physiologically scaled tissue implants[228]. Overall, the selected crosslinking method for PBHs bioprinting impacts cellular viability and behavior, and the application should be considered while selecting the appropriate technique[29,229-231].

Printed droplets do not merge in these constructs, thereby increasing their mechanical stability. In addition to enhanced cellular functions, physical crosslinking produces no toxic byproducts and contributes to rapid gelation[232]. Notably, the plasma membrane can initially become damaged at low points in cells printed with low fluences and short gelation time, but the cells will recover rapidly through the sealing mechanism[233]. Consequently, despite providing a cushioning effect, all polymer concentrations require a suitable gelation time[234]. If the encapsulation process fails, the cells will not adhere to the scaffold and proliferate on the well plate instead; consequently, the cells are not able to be 3D cultivated[195,235].

For bioprinting, Visscher *et al.*[236] developed cartilage-derived decellularized ECM-based photo-crosslinkable porcine auricular cartilage hydrogels/methacrylate (cdECMMA). Subsequent to the printing, cdECM-based constructs were chemically modified by methacrylate reactions, providing structural integrity. Moreover, the bioink was prepared with a solution consisting of 37.5 mg/mL gelatin type A, 3 mg/mL HA, and photoinitiator (0.1% v/v, Irgacure 2959). A UV light intensity of 200 mW/cm^2 was used for 2 min to induce photo-crosslinking in this bioink formulation, and various concentrations (20, 30, and 40 mg/mL) of cdECMMA hydrogels were produced. With the increment of cdECMMA concentrations, the hydrogels' stiffness was considerably enhanced (20 mg/mL: 3837 ± 462 Pa, 30 mg/mL: 10381 ± 1339 Pa, and 40 mg/mL: 25,050 ± 2573 Pa). In addition, all cdECMMA constructs'

concentrations showed viability greater than 90% (1, 3, and 7 days). Therefore, they demonstrated that the photo-crosslinkable cdECM-based bioinks could be successfully engineered for auricular cartilage reconstruction while exhibiting favorable printability and structural stability.

Toward the same goal, cartilage acellular matrix (CAM) bioinks containing silk fibroin were engineered for bioprinting from porcine cartilage by a team of scientists[237]. In the first step, CAM-silk scaffolds were crosslinked with methanol only, 100 mM 1-ethyl-3-(-3-dimethylaminopropyl) carbodiimide/N-hydroxysuccinimide (EDC/NHS) in water (EDC-W), or 80% methanol (EDC-M) for 12 h. Subsequent to incubation for 7 days in collagenase, the printed CAM-silk scaffolds illustrated significant changes in shape and weight. A non-crosslinked CAM-silk scaffold collapsed after 1 day of treatment with collagenase 0.2%. At the end of incubation period, the extruded structures completely dissolved, and the methanol- and EDC-W-treated groups displayed analogous degradation characteristics after 3 to 5 days. In contrast, EDC-M could preserve the printed scaffolds well. The EDC-M-treated scaffolds did not degrade after 7 days, and EDC-W scaffolds retained ~20% of their initial weight.

5. Challenges and perspectives

Within the context of bioprinting approaches, classified based on the cells format and the number of cells generated during the bioprinting process, an unmet need still exists, which is related to the cell damage due to the shear stress during the bioprinting procedure. Furthermore, bioinks with enhanced cell shielding features are not largely explored. In this regard, scholars are merging experimental investigations with probabilistic models to improve our understanding of how cells get encapsulated into droplets in bioprinting and develop novel bioinks having the right balance of rheological characteristics for stress shielding and printability. The applications of the present single-cell bioprinting techniques are limited owing to multiple issues. To begin with, although the efficiency and reliability of the single-cell encapsulation are significantly improved, the single-cell printing's overall throughput is still low. Secondly, current printing methods typically rely on the single-cell droplets' printing within an open environment, causing deviation and interference in the following analysis. In other methods of bioprinting, one major obstacle is associated with reproducing a highly complex set of cell–matrix and cell–cell interactions, which are needed to guarantee sufficient organ functions. Besides, some of the developed bioinks containing several populations of cells have failed to replicate the native ECM microenvironment in the body, a bottleneck that remains to be addressed. Concerning the perspectives of bioprinting strategies, engineering a print head or a hand-held printer with digital control for direct tissue repair is one of the promising clinical applications. Indeed, via utilizing the scanned lesions' 3D reconstructions, bioprinting is capable of accurately delivering GFs, cells, and biomaterial-based scaffolds to repair the lesion with different thicknesses and shapes. Equipping bioprinters with microfluidic printing heads can also enable smooth and rapid switching across various bioink reservoirs in the printing process, making it simpler in order to recapitulate the native tissues' biological intricacy. Another point that should be considered in the bioprinting is the design of a gradient scaffold that can be seamlessly transferred from the cartilage layer to the bone layer while maintaining the distinct properties and functions of each tissue. This has made some progress, but more efforts are needed, especially with merging bioprinting technologies and co-bioprinting of several bioinks. Moreover, the practicability and commercial availability of bioinks and cells should be considered, including their cost, source, shelf-life, and approval by the Food and Drug Administration (FDA). Another direction is combining bioprinting techniques to meet different current obstacles, which is grabbing considerable attention among scientists. For instance, the employment of bioprinting approaches with diverse resolutions can be used to imitate the aspects of natural biological systems, which are operating on various scales. Moreover, evaluating the cellular functions after and during bioprinting will benefit the broad applicability and future success of bioprinting strategies. Last but not least, the continual optimization of bioprinting factors, the evolution of bioprinting equipment like imaging used for single-cell sorting, and the modification of bioink formulations like cellular density are ongoing trends to make bioprinting approaches more advanced, precise, and relevant to certain requirements.

Protein-based materials are among the most promising sources for the bioinks' formulations utilized in bioprinting strategies. Nonetheless, as with all the materials that are developed from biologics, there can be batch-to-batch variations in these materials, and thus the bioinks made from them. Hence, it is of cardinal importance to establish well-defined and strict protocols for the concentration, purification, and extraction of the employed proteins to provide reliable and reproducible outcomes. Additionally, selecting the best accessible method of sterilization can serve an essential role in guaranteeing the final bioink's safety and ideal properties. On the one hand, proteins originating from xenogeneic sources represent a potential ethical concern and could increase the risk of pathogen transmission. On the other hand, allogeneic sources of proteins pose extra difficulty in the source material's availability, particularly taking into account

the regulations on tissue and organ donation specific to each of the countries. All in all, a shift toward allogeneic sourcing necessitates collaboration among research groups, companies, and regulatory bodies in defining more standardized regulations on tissue and organ donation. Besides, biological, physical, and biochemical requirements of cartilage and bone tissues in designing PBHs are sometimes overlooked, representing an issue that should be addressed in order to obtain accurate experimental results in this field.

Natural proteins, including collagen, gelatin, silk fibroin, fibrin, keratin, elastin, and resilin, are in the spotlight of investigations on PBHs. However, each displays several drawbacks that should be overcome to achieve favorable outcomes. In the case of collagen-based bioinks, bioprinting of pure collagen is rather complex because of its low viscosity; a suggested solution in this regard is combining it with viscous polymers. Additionally, to enhance its shape fidelity, physical crosslinking and blending with other polymers can be employed. Other hindrances in the bioprinting of collagen that need to be addressed are poor mechanical strength and rapid hydrolysis. A common problem of pure gelatin bioinks at physiological temperature is their low viscosity, which can be also improved when blending them with viscous polymers. Another obstacle, again solvable via combining with other polymers, is associated with the low bioprinting resolution of these bioinks. Notably, to augment their poor shape fidelity, post-printing crosslinking and utilizing external support for the bioinks have been demonstrated as effective methods. Unfortunately, the stress shielding features of gelatin bioinks are low; a complication that can be tackled by nozzle temperature optimization during bioprinting to increase cellular survival. Pure silk bioinks have the disadvantage of high viscosity, resulting in nozzle clogging at the time of bioprinting; one efficacious strategy involves using recombinant silk that possesses lower viscosity compared to that of the native silk. Furthermore, lacking cell binding domains which can limit cellular attachment, low cellular growth and function support, and the absence of an established protocol for the optimization of silk-based bioinks are other obstacles that need to be taken into account. Particularly, scholars should address the high rate of enzymatic degradation and poor mechanical parameters related to the silk fibroin bioinks as well as the weak structural integrity associated with the silk sericin bioinks. The chief challenge of employing fibrin as a bioink is its irreversible and rapid gelation at the body temperature, making its bioprinting intricate. As an alternative, fibrinogen and thrombin blends can be printed together at low temperatures in order to inhibit early crosslinking. The fast degradation of fibrin bioinks is another problem impairing their capability to form stable constructs; this matter can be solved by blending them with other biopolymers. Besides, the fundamental challenges in bioprinting of keratin, elastin, and resilin are poor extensibility, possibility of contaminations after the purification process, and difficulty in determining the molecular sequence and primary sequence of resilin owing to the diminished stability during the purification.

Despite the rapid advances of bioprinting approaches in recent years, the above-mentioned obstacles should be surmounted to move this field forward. Regarding the PBHs, successful examples on the development of cartilage- and bone-engineered constructs employing bioprinting strategies have been described. As stated, several factors, including biophysical and biochemical parameters, and PBHs' process considerations must be taken into account, and multiple challenges with respect to these subjects are required to be overcome to ultimately translate these concepts into clinics in the foreseeable future.

6. Conclusion

In bioprinting, there is a paramount need to address the cell damage caused by shear stress and to develop bioinks with ideal cell protection. Researchers have been employing experimental investigations and probabilistic models to understand cell encapsulation in droplets and to design bioinks with suitable characteristics. Notably, current single-cell bioprinting techniques have limitations in terms of throughput and deviation in the printing process. In addition, reproducing complex cell–matrix and cell–cell interactions is a significant challenge for other bioprinting methods. Future directions include developing tissue repair printers, equipping bioprinters with microfluidic heads, and designing gradient scaffolds. Of note, combining different bioprinting approaches, evaluating cellular functions, and optimizing factors like imaging and bioink formulations are ongoing trends to advance the bioprinting field. Protein-based materials display promise for bioinks but may have batch-to-batch variations. It is important to mention that establishing strict protocols for protein concentration, purification, and extraction is crucial to ensure reliable and reproducible outcomes in bioprinting. Selecting the best method of sterilization is also critical for the safety and properties of the final bioink. In addition, ethical concerns and pathogen transmission risks arise when using proteins from xenogeneic sources, while allogeneic sources are limited in availability due to regulations on tissue and organ donation. In this regard, a collaboration between research groups, companies, and regulatory bodies is required to standardize regulations on tissue and organ donation for allogeneic sourcing. Natural proteins such

as collagen, gelatin, silk fibroin, fibrin, keratin, elastin, and resilin have drawbacks that need to be addressed for favorable outcomes in bioprinting. In general, significant advancements have been made in bioprinting, but there are still obstacles to overcome in order to move the field forward. Successful examples of utilizing bioprinting for cartilage and bone TE have been discussed; nevertheless, there are multiple parameters and bottlenecks that should be paid attention to. Biophysical and biochemical factors, as well as considerations for process optimization, must be taken into account. All in all, tackling the mentioned challenges will ultimately lead to translating bioprinting concepts into clinical applications in the near future.

Acknowledgments

None.

Funding

This work was supported by Alexander von Humboldt Foundation (Fellowship to F.G.), the Outstanding Clinical Discipline Project of Shanghai Pudong (Grant No. PWYgy2021-08), the Pudong New Area Traditional Chinese Medicine Science and Technology Innovation project (PDZY-2020-0607), the Young Medical Talents Training Program of Pudong Health Committee of Shanghai (Grant No. PWRq 2021-08), the Health Industry Clinical Research Project of Shanghai Health Commission (Grant No. 20224Y0393), and the National Natural Science Foundation of China (Grant No. 81971753, 82170897).

Conflict of interest

The authors certify that they have no affiliations with, or involvement in, any organization or entity with any financial interest or non-financial interest in the subject matter or materials discussed in this manuscript. All authors have read and agreed to the published version of the manuscript.

Author contributions

Conceptualization: Behafarid Ghalandari, Baoqing Yu, Farnaz Ghorbani

Funding acquisition: Behafarid Ghalandari, Baoqing Yu, Farnaz Ghorbani

Supervision: Behafarid Ghalandari, Baoqing Yu, Farnaz Ghorbani

Visualization: Mehran Khajehmohammadi

Writing – original draft: Mehran Khajehmohammadi, Negar Bakhtiary, Niyousha Davari, Soulmaz Sarkari, Hamidreza Tolabi, Dejian Li

Writing – review & editing: Behafarid Ghalandari, Farnaz Ghorbani

Ethics approval and consent to participate

Not applicable.

Consent for publication

Not applicable.

Availability of Data

The resources that support this review work are available upon request from the corresponding author.

References

1. Ozbolat IT, 2017, Bioprinting of osteochondral tissues: A perspective on current gaps and future trends. *Int J Bioprint,* 3(2).

   http://doi:10.18063/IJB.2017.02.007

2. Deng C, Chang J, Wu C, 2019, Bioactive scaffolds for osteochondral regeneration. *J Orthop Transl,* 17: 15–25.

   http://doi:10.1016/j.jot.2018.11.006

3. Gonçalves AM, Moreira A, Weber A, *et al.*, 2021, Costa, osteochondral tissue engineering: The potential of electrospinning and additive manufacturing. *Pharmaceutics*, 13(7): 983.

   http://doi:10.3390/pharmaceutics13070983

4. Moris H, Ghaee A, Karimi M, *et al.*, 2022, Preparation and characterization of Pullulan-based nanocomposite scaffold incorporating Ag-Silica Janus particles for bone tissue engineering. *Biomater Adv,* 135: 212733.

   http://doi:10.1016/j.bioadv.2022.212733

5. Ghorbani F, Ghalandari B, Khan AL, *et al.*, 2020, Decoration of electrical conductive polyurethane-polyaniline/polyvinyl alcohol matrixes with mussel-inspired polydopamine for bone tissue engineering. *Biotechnol Prog,* 36(6): e3043.

   http://doi:10.1002/btpr.3043

6. Ghorbani F, Zamanian A, Sahranavard M, 2019, Mussel-inspired polydopamine-mediated surface modification of freeze-cast poly (ε-caprolactone) scaffolds for bone tissue engineering applications. *Biomed Eng/Biomed Tech,* 65(3): 273–287.

   http://doi:10.1515/bmt-2019-0061

7. Sahranavard M, Zamanian A, Ghorbani F, *et al.*, 2020, A critical review on three dimensional-printed chitosan hydrogels for development of tissue engineering. *Bioprinting*, 17: e00063.

   http://doi:10.1016/j.bprint.2019.e00063

8. Yilmaz B, Al Rashid A, Mou YA, *et al.*, 2021, Bioprinting: A review of processes, materials and applications. *Bioprinting*, 23: e00148.

   https://doi.org/10.1016/j.bprint.2021.e00148

9. Ding S, Feng L, Wu J, *et al.*, 2018, Bioprinting of stem cells : Interplay of bioprinting process, bioinks, and stem cell properties. *ACS Biomater Sci Eng*, 4(9): 3108–3124.

   http://doi:10.1021/acsbiomaterials.8b00399

10. Kundu J, Shim J-H, Jang J, *et al.*, 2015, An additive manufacturing-based PCL-alginate-chondrocyte bioprinted scaffold for cartilage tissue engineering. *J Tissue Eng Regen Med,* 9(11): 1286–1297.

    http://doi:10.1002/term.1682

11. Ozbolat IT, 2015, Bioprinting scale-up tissue and organ constructs for transplantation. *Trends Biotechnol,* 33(7): 395–400.

    http://doi:10.1016/j.tibtech.2015.04.005

12. Kačarević Ž, Rider P, Alkildani S, *et al.*, 2018, An introduction to 3D bioprinting: Possibilities, challenges and future aspects. *Materials (Basel)*, 11(11): 2199.

    http://doi:10.3390/ma11112199

13. Ghorbani F, Ghalandari B, Khajehmohammadi M, *et al.*, 2023, Photo-cross-linkable hyaluronic acid bioinks for bone and cartilage tissue engineering applications. *Int Mater Rev,* 68(6): 1–42.

    http://doi:10.1080/09506608.2023.2167559

14. Raza F, Zafar H, Zhu Y, *et al.*, 2018, A review on recent advances in stabilizing peptides/proteins upon fabrication in hydrogels from biodegradable polymers. *Pharmaceutics*, 10(1): 16.

    http://doi:10.3390/pharmaceutics10010016

15. Di Bella C, Fosang A, Donati DM, *et al.*, 2015, 3D bioprinting of cartilage for orthopedic surgeons : Reading between the lines. *Front Surg*, 2: 1–7.

    http://doi:10.3389/fsurg.2015.00039

16. Tolabi H, Davari N, Khajehmohammadi M, *et al.*, 2023, Progress of microfluidic hydrogel-based scaffolds and organ-on-chips for the cartilage tissue engineering. *Adv Mater,* 35(26): 2208852.

    http://doi:10.1002/adma.202208852

17. Razaviye MK, Tafti RA, Khajehmohammadi M, 2022, An investigation on mechanical properties of PA12 parts produced by a SLS 3D printer: An experimental approach. *CIRP J Manuf Sci Technol,* 38: 760–768.

    http://doi:10.1016/j.cirpj.2022.06.016

18. Dababneh AB, Ozbolat IT, 2014, Bioprinting technology: A current state-of-the-art review. *J Manuf Sci Eng Trans ASME,* 136(6): 1–12.

    http://doi:10.1115/1.4028512

19. Khajehmohammadi M, Azizi Tafti R, Nikukar H, 2023, Effect of porosity on mechanical and biological properties of bioprinted scaffolds. *J Biomed Mater Res Part A,* 111(2): 245–260.

    http://doi:10.1002/jbm.a.37455

20. Schloss AC, Williams DM, Regan LJ, 2016, Protein-based hydrogels for tissue engineering. *Adv Exp Med Biol,* 940: 167–177.

    http://doi:10.1007/978-3-319-39196-0_8

21. Davari N, Bakhtiary N, Khajehmohammadi M, *et al.*, 2022, Protein-based hydrogels: Promising materials for tissue engineering. *Polymers (Basel)*, 14: 986.

    http://doi:10.3390/polym14050986

22. Rasheed T, Bilal M, Zhao Y, *et al.*, 2019, Physiochemical characteristics and bone/cartilage tissue engineering potentialities of protein-based macromolecules — A review. *Int J Biol Macromol*, 121(5): 13–22.

    http://doi:10.1016/j.ijbiomac.2018.10.009

23. Catoira MC, Fusaro L, Di Francesco D, *et al.*, 2019, Overview of natural hydrogels for regenerative medicine applications. *J Mater Sci Mater Med,* 30(10): 115.

    http://doi:10.1007/s10856-019-6318-7

24. Maia FRA, Oliveira JM, Reis RL, eds., 2023, *Handbook of the Extracellular Matrix*, Springer International Publishing, Cham.

    http://doi:10.1007/978-3-030-92090-6

25. Włodarczyk-Biegun MK, del Campo A, 2017, 3D bioprinting of structural proteins. *Biomaterials*, 134: 180–201.

    http://doi:10.1016/j.biomaterials.2017.04.019

26. Lotfi Z, Khakbiz M, Davari N, *et al.*, 2023, Fabrication and multiscale modeling of polycaprolactone/amniotic membrane electrospun nanofiber scaffolds for wound healing. *Artif Organs*, 00: 1–18.

    http://doi:10.1111/aor.14518

27. Norouzi F, Pourmadadi M, Yazdian F, *et al.*, 2022, PVA-based nanofibers containing chitosan modified with graphene oxide and carbon quantum dot-doped TiO2 enhance wound healing in a rat model. *J Funct Biomater*, 13(4): 300.

    http://doi:10.3390/jfb13040300

28. Yahay Z, Tolabi H, Delavar F, *et al.*, 2023, Fabrication of meso/macroporous TiO2/PCL composite scaffolds by direct ink writing: The effects of porogen content on the compressive modulus and in vitro behavior. *Mater Today Commun,* 35: 105769.

    http://doi:10.1016/j.mtcomm.2023.105769

29. Veiga A, Silva IV, Duarte MM, *et al.*, 2021, Current trends on protein driven bioinks for 3D printing. *Pharmaceutics*, 13(9): 1444.

    http://doi:10.3390/pharmaceutics13091444

30. Khoeini R, Nosrati H, Akbarzadeh A, *et al.*, 2021, Natural and synthetic bioinks for 3D bioprinting. *Adv NanoBiomed Res,* 1(8): 2000097.

    http://doi:10.1002/anbr.202000097

31. Abascal NC, Regan L, 2018, The past, present and future of protein-based materials. *Open Biol,* 8(10): 180113.

http://doi:10.1098/rsob.180113

32. Jeshvaghani PA, Pourmadadi M, Yazdian F, *et al.*, 2023, Synthesis and characterization of a novel, pH-responsive sustained release nanocarrier using polyethylene glycol, graphene oxide, and natural silk fibroin protein by a green nano emulsification method to enhance cancer treatment. *Int J Biol Macromol,* 226: 1100–1115.

http://doi:10.1016/j.ijbiomac.2022.11.226

33. Hajiabbas M, Okoro OV, Delporte C, *et al.*, 2023, Proteins and polypeptides as biomaterials inks for 3D printing, in *Handbook of the Extracellular Matrix*, Springer International Publishing, Cham, 2023, 1–34.

http://doi:10.1007/978-3-030-92090-6_15-1

34. Gagner JE, Kim W, Chaikof EL, 2014, Designing protein-based biomaterials for medical applications. *Acta Biomater*, 10(4): 1542–1557.

http://doi:10.1016/j.actbio.2013.10.001

35. Lee A, Hudson AR, Shiwarski DJ, *et al.*, 2019, 3D bioprinting of collagen to rebuild components of the human heart. *Science*, 365(6452): 482–487.

http://doi:10.1126/science.aav9051

36. Łabowska MB, Cierluk K, Jankowska AM, *et al.*, 2021, A review on the adaption of alginate-gelatin hydrogels for 3D cultures and bioprinting. *Materials (Basel)*, 14(4): 858.

http://doi:10.3390/ma14040858

37. Liu S, Yu J-M, Gan Y-C, *et al.*, 2023, Biomimetic natural biomaterials for tissue engineering and regenerative medicine: New biosynthesis methods, recent advances, and emerging applications. *Mil Med Res,* 10(1): 16.

http://doi:10.1186/s40779-023-00448-w

38. Cheung H-Y, Lau K-T, Lu T-P, *et al.*, 2007, A critical review on polymer-based bio-engineered materials for scaffold development. *Compos Part B Eng,* 38(3): 291–300.

http://doi:10.1016/j.compositesb.2006.06.014

39. Al Enezy-Ulbrich MA, Malyaran H, Lange RD, *et al.*, 2020, Impact of reactive amphiphilic copolymers on mechanical properties and cell responses of fibrin-based hydrogels. *Adv Funct Mater,* 30(38): 2003528.

http://doi:10.1002/adfm.202003528

40. Vernerey FJ, Greenwald EC, Bryant SJ, 2012, Triphasic mixture model of cell-mediated enzymatic degradation of hydrogels. *Comput Methods Biomech Biomed Engin,* 15(11): 1197–1210.

http://doi:10.1080/10255842.2011.585973

41. Khan F, Atif M, Haseen M, *et al.*, 2022, Synthesis, classification and properties of hydrogels: Their applications in drug delivery and agriculture. *J Mater Chem B,* 10(2): 170–203.

http://doi:10.1039/D1TB01345A

42. Chakraborty J, Ghosh S, 2020, Cellular proliferation, self-assembly, and modulation of signaling pathways in silk fibroin gelatin-based 3D bioprinted constructs. *ACS Appl Bio Mater,* 3(12): 8309–8320.

http://doi:10.1021/acsabm.0c01252

43. Bakhtiary N, Ghalandari B, Ghorbani F, *et al.*, 2023, Advances in peptide-based hydrogel for tissue engineering. *Polymers (Basel)*, 15(5): 1068.

http://doi:10.3390/polym15051068

44. Huettner N, Dargaville TR, Forget A, 2018, Discovering cell-adhesion peptides in tissue engineering: Beyond RGD. *Trends Biotechnol*, 36(4): 372–383.

http://doi:10.1016/j.tibtech.2018.01.008

45. Gao G, Cui X, Bone BÁ, *et al.*, 2016, Three-dimensional bioprinting in tissue engineering and regenerative medicine. *Biotechnol Lett,* 38: 422–434.

http://doi:10.1007/s10529-015-1975-1

46. Tasoglu S, Demirci U, 2013, Bioprinting for stem cell research. *Trends Biotechnol*, 31(1): 10–19.

http://doi:10.1016/j.tibtech.2012.10.005

47. Riba J, Renz N, Niemöller C, *et al.*, 2016, Molecular genetic characterization of individual cancer cells isolated via single-cell printing. *PLoS One,* 11(9): e0163455.

http://doi:10.1371/journal.pone.0163455

48. Stumpf F, Schoendube J, Gross A, *et al.*, 2015, Single-cell PCR of genomic DNA enabled by automated single-cell printing for cell isolation. *Biosens Bioelectron,* 69: 301–306.

http://doi:10.1016/j.bios.2015.03.008

49. Zhang X, Wei X, Wei Y, *et al.*, 2020, The up-to-date strategies for the isolation and manipulation of single cells. *Talanta,* 218: 121147.

http://doi:10.1016/j.talanta.2020.121147

50. Herzenberg LA, Parks D, Sahaf B, *et al.*, 2002, The history and future of the fluorescence activated cell sorter and flow cytometry: A view from stanford. *Clin Chem,* 48(10): 1819–1827.

http://doi:10.1093/clinchem/48.10.1819

51. Zhou Y, Shaw D, Lam C, *et al.*, 2018, Beating the odds: The poisson distribution of all input cells during limiting dilution grossly underestimates whether a cell line is clonally-derived or not. *Biotechnol Prog,* 34(3): 559–569.

http://doi:10.1002/btpr.2560

52. Gross A, Schoendube J, Zimmermann S, *et al.*, 2015, Technologies for single-cell isolation. *Int J Mol Sci,* 16(8): 16897–16919.

http://doi:10.3390/ijms160816897

53. Zhang X, Li T, Liu F, *et al.*, 2019, Comparative analysis of droplet-based ultra-high-throughput single-cell RNA-Seq systems. *Mol Cell,* 73(1): 130–142.e5.

http://doi:10.1016/j.molcel.2018.10.020

54. Matuła K, Rivello F, Huck WTS, 2020, Single-cell analysis using droplet microfluidics. *Adv Biosyst,* 4(1): 1900188.

http://doi:10.1002/adbi.201900188

55. Klein AM, Mazutis L, Akartuna I, *et al.*, 2015, Droplet barcoding for single-cell transcriptomics applied to embryonic stem cells. *Cell,* 161(5): 1187–1201.

http://doi:10.1016/j.cell.2015.04.044

56. Han X, Wang R, Zhou Y, *et al.*, 2018, Mapping the mouse cell atlas by microwell-seq. *Cell,* 172(5): 1091–1107.e17.

http://doi:10.1016/j.cell.2018.02.001

57. Rettig JR, Folch A, 2005, Large-scale single-cell trapping and imaging using microwell arrays. *Anal Chem,* 77(17): 5628–5634.

http://doi:10.1021/ac0505977

58. Zhou Y, Basu S, Wohlfahrt KJ, *et al.*, 2016, A microfluidic platform for trapping, releasing and super-resolution imaging of single cells. *Sensors Actuators B Chem*, 232: 680–691.

http://doi:10.1016/j.snb.2016.03.131

59. Tan W-H, Takeuchi S, 2007, A trap-and-release integrated microfluidic system for dynamic microarray applications. *Proc Natl Acad Sci,* 104(4): 1146–1151.

http://doi:10.1073/pnas.0606625104

60. Calvert P, 2007, Printing cells. *Science*, 318(5848): 208–209.

http://doi:10.1126/science.1144212

61. Yusof A, Keegan H, Spillane CD, *et al.*, 2011, Inkjet-like printing of single-cells. *Lab Chip*, 11(14): 2447.

http://doi:10.1039/c1lc20176j

62. Wang Y, Wang X, Pan T, *et al.*, 2021, Label-free single-cell isolation enabled by microfluidic impact printing and real-time cellular recognition. *Lab Chip,* 21(19): 3695–3706.

http://doi:10.1039/D1LC00326G

63. Schoendube J, Wright D, Zengerle R, *et al.*, 2015, Single-cell printing based on impedance detection. *Biomicrofluidics,* 9(1): 014117.

http://doi:10.1063/1.4907896

64. Nagai M, Kato K, Soga S, *et al.*, 2020, Scalable parallel manipulation of single cells using micronozzle array integrated with bidirectional electrokinetic pumps. *Micromachines,* 11(4): 442.

http://doi:10.3390/mi11040442

65. Feng L, Sun Y, Ohsumi C, *et al.*, 2013, Accurate dispensing system for single oocytes using air ejection. *Biomicrofluidics,* 7(5): 054113.

http://doi:10.1063/1.4824394

66. Demirci U, Montesano G, 2007, Single cell epitaxy by acoustic picolitre droplets. *Lab Chip,* 7(9): 1139.

http://doi:10.1039/b704965j

67. Guo F, Mao Z, Chen Y, *et al.*, 2016, Three-dimensional manipulation of single cells using surface acoustic waves. *Proc Natl Acad Sci,* 113(6): 1522–1527.

http://doi:10.1073/pnas.1524813113

68. Bertassoni LE, 2022, Bioprinting of complex multicellular organs with advanced functionality—recent progress and challenges ahead. *Adv Mater,* 34(3): 2101321.

http://doi:10.1002/adma.202101321

69. Daly AC, Prendergast ME, Hughes AJ, *et al.*, 2021, Bioprinting for the biologist. *Cell,* 184(1): 18–32.

http://doi:10.1016/j.cell.2020.12.002

70. Barron JA, Krizman DB, Ringeisen BR, 2005, Laser printing of single cells: Statistical analysis, cell viability, and stress. *Ann Biomed Eng*, 33(2): 121–130.

http://doi:10.1007/s10439-005-8971-x

71. Yamaguchi S, Ueno A, Akiyama Y, *et al.*, 2012, Cell patterning through inkjet printing of one cell per droplet. *Biofabrication*, 4(4): 045005.

http://doi:10.1088/1758-5082/4/4/045005

72. Zhang K, Chou C-K, Xia X, *et al.*, 2014, Block-cell-printing for live single-cell printing. *Proc Natl Acad Sci,* 111(8): 2948–2953.

http://doi:10.1073/pnas.1313661111

73. Zhou X, Wu H, Wen H, *et al.*, 2022, Advances in single-cell printing. *Micromachines*, 13(1): 80.

http://doi:10.3390/mi13010080

74. Murphy SV, De Coppi P, Atala A, 2020, Opportunities and challenges of translational 3D bioprinting. *Nat Biomed Eng,* 4(4): 370–380.

http://doi:10.1038/s41551-019-0471-7

75. Zhang P, Abate AR, 2020, High-definition single-cell printing: Cell-by-cell fabrication of biological structures. *Adv Mater,* 32(52): 2005346.

http://doi:10.1002/adma.202005346

76. Hong S, Lee JY, Hwang C, *et al.*, 2016, Inhibition of Rho-associated protein kinase increases the angiogenic potential of mesenchymal stem cell aggregates via paracrine effects. *Tissue Eng Part A,* 22(3-4): 233–243.

http://doi:10.1089/ten.tea.2015.0289

77. Lei J, Trevino E, Temenoff J, 2016, Cell number and chondrogenesis in human mesenchymal stem cell aggregates is affected by the sulfation level of heparin used as a cell coating. *J Biomed Mater Res Part A,* 104(7): 1817–1829.

http://doi:10.1002/jbm.a.35713

78. Lin R-Z, Chang H-Y, 2008, Recent advances in three-dimensional multicellular spheroid culture for biomedical research. *Biotechnol J,* 3(9-10): 1172–1184.

http://doi:10.1002/biot.200700228

79. Derby B, 2012, Printing and prototyping of tissues and scaffolds. *Science*, 338(6109): 921–926.

http://doi:10.1126/science.1226340

80. Marga F, Jakab K, Khatiwala C, *et al.*, 2012, Toward engineering functional organ modules by additive manufacturing. *Biofabrication*, 4(2): 022001.

http://doi:10.1088/1758-5082/4/2/022001

81. Marchioli G, van Gurp L, van Krieken PP, *et al.*, 2015, Fabrication of three-dimensional bioplotted hydrogel scaffolds for islets of Langerhans transplantation. *Biofabrication*, 7(2): 025009.

http://doi:10.1088/1758-5090/7/2/025009

82. Tan Y, Richards DJ, Trusk TC, *et al.*, 2014, 3D printing facilitated scaffold-free tissue unit fabrication. *Biofabrication*, 6(2): 024111.

http://doi:10.1088/1758-5082/6/2/024111

83. Yang X, Sun Y, Wang Q, 2013, A phase field approach for multicellular aggregate fusion in biofabrication. *J Biomech Eng,* 135: 071005.

http://doi:10.1115/1.4024139

84. Yang X, Mironov V, Wang Q, 2012, Modeling fusion of cellular aggregates in biofabrication using phase field theories. *J Theor Biol,* 303: 110–118.

http://doi:10.1016/j.jtbi.2012.03.003

85. Mironov V, Visconti RP, Kasyanov V, *et al.*, 2009, Organ printing: Tissue spheroids as building blocks. *Biomaterials*, 30(12): 2164–2174.

http://doi:10.1016/j.biomaterials.2008.12.084

86. Keriquel V, Oliveira H, Rémy M, *et al.*, 2017, In situ printing of mesenchymal stromal cells, by laser-assisted bioprinting, for in vivo bone regeneration applications. *Sci Rep,* 7(1): 1778.

http://doi:10.1038/s41598-017-01914-x

87. Adhikari J, Perwez MS, Das A, *et al.*, 2021, Development of hydroxyapatite reinforced alginate–chitosan based printable biomaterial-ink. *Nano-Structures Nano-Objects*, 25: 100630.

http://doi:10.1016/j.nanoso.2020.100630

88. Ozbolat IT, Hospodiuk M, 2016, Current advances and future perspectives in extrusion-based bioprinting. *Biomaterials,* 76: 321–343.

http://doi:10.1016/j.biomaterials.2015.10.076

89. Kim SH, Yeon YK, Lee JM, *et al.*, 2018, Precisely printable and biocompatible silk fibroin bioink for digital light processing 3D printing. *Nat Commun,* 9(1): 1–14.

http://doi:10.1038/s41467-018-03759-y

90. Mandrycky C, Wang Z, Kim K, *et al.*, 2016, 3D bioprinting for engineering complex tissues. *Biotechnol Adv,* (4).

http://doi:10.1016/j.biotechadv.2015.12.011

91. Ren X, Wang F, Chen C, *et al.*, 2016, Engineering zonal cartilage through bioprinting collagen type II hydrogel constructs with biomimetic chondrocyte density gradient. *BMC Musculoskelet Disord,* 17(1): 1–10.

http://doi:10.1186/s12891-016-1130-8

92. Kesti M, Eberhardt C, Pagliccia G, *et al.*, 2015, Bioprinting complex cartilaginous structures with clinically compliant biomaterials. *Adv Funct Mater,* 25(48): 7406–7417.

http://doi:10.1002/adfm.201503423

93. López-Marcial GR, Zeng AY, Osuna C, *et al.*, 2018, Agarose-based hydrogels as suitable bioprinting materials for tissue engineering. *ACS Biomater Sci Eng*, 4(10): 3610–3616.

http://doi:10.1021/acsbiomaterials.8b00903

94. Luo Y, Luo G, Gelinsky M, *et al.*, 2017, 3D bioprinting scaffold using alginate/polyvinyl alcohol bioinks. *Mater Lett,* 189: 295–298.

http://doi:10.1016/j.matlet.2016.12.009

95. Asohan AW, Hashim R, Ku Ishak KM, *et al.*, 2022, Preparation and characterisation of cellulose nanocrystal/alginate/polyethylene glycol diacrylate (CNC/Alg/PEGDA) hydrogel using double network crosslinking technique for bioprinting application. *Appl Sci,* 12(2): 771.

http://doi:10.3390/app12020771

96. Hong S, Sycks D, Chan HF, *et al.*, 2015, 3D printing of highly stretchable and tough hydrogels into complex, cellularized structures. *Adv Mater,* 27(27): 4035–4040.

http://doi:10.1002/adma.201501099

97. Kosik-Kozioł A, Costantini M, Bolek T, *et al.*, 2017, PLA short sub-micron fiber reinforcement of 3D bioprinted alginate constructs for cartilage regeneration. *Biofabrication*, 9(4): 044105.

http://doi:10.1088/1758-5090/aa90d7

98. Bakhtiary N, Liu C, Ghorbani F, 2021, Bioactive inks development for osteochondral tissue engineering: A mini-review. *Gels*, 7(4): 274.

http://doi:10.3390/gels7040274

99. Das S, Pati F, Choi Y-J, *et al.*, 2015, Bioprintable, cell-laden silk fibroin–gelatin hydrogel supporting multilineage differentiation of stem cells for fabrication of three-dimensional tissue constructs. *Acta Biomater*, 11: 233–246.

http://doi:10.1016/j.actbio.2014.09.023

100. Duan B, Kapetanovic E, Hockaday LAA, *et al.*, 2014, Three-dimensional printed trileaflet valve conduits using biological hydrogels and human valve interstitial cells. *Acta Biomater,* 10(5): 1836–1846.

http://doi:10.1016/j.actbio.2013.12.005

101. Murphy SV, Skardal A, Atala A, 2013, Evaluation of hydrogels for bio-printing applications. *J Biomed Mater Res - Part A,* 101(1): 272–284.

http://doi:10.1002/jbm.a.34326

102. Williams D, Thayer P, Martinez H, *et al.*, 2018, A perspective on the physical, mechanical and biological specifications of bioinks and the development of functional tissues in 3D bioprinting. *Bioprinting*, 9: 19–36.

http://doi:10.1016/j.bprint.2018.02.003

103. Tolabi H, Bakhtiary N, Sayadi S, *et al.*, 2022, A critical review on polydopamine surface-modified scaffolds in musculoskeletal regeneration. *Front Bioeng Biotechnol,* 10: 1008360.

http://doi:10.3389/fbioe.2022.1008360

104. Diamantides N, Wang L, Pruiksma T, *et al.*, 2017, Correlating rheological properties and printability of collagen bioinks: The effects of riboflavin photocrosslinking and pH. *Biofabrication*, 9(4): 034102.

http://doi:10.1088/1758-5090/aa780f

105. Moncal KK, Ozbolat V, Datta P, *et al.*, 2019, Thermally-controlled extrusion-based bioprinting of collagen. *J Mater Sci Mater Med,* 30(5): 55.

http://doi:10.1007/s10856-019-6258-2

106. Rhee S, Puetzer JL, Mason BN, *et al.*, 2016, 3D bioprinting of spatially heterogeneous collagen constructs for cartilage tissue engineering. *ACS Biomater Sci Eng,* 2(10): 1800–1805.

http://doi:10.1021/acsbiomaterials.6b00288

107. Leucht A, Volz A-C, Rogal J, *et al.*, 2020, Advanced gelatin-based vascularization bioinks for extrusion-based bioprinting of vascularized bone equivalents. *Sci Rep,* 10(1): 5330.

http://doi:10.1038/s41598-020-62166-w

108. Osidak EO, Kozhukhov VI, Osidak MS, 2020, Collagen as bioink for bioprinting: A comprehensive review. *Int J Bioprint,* 6(3): 270.

http://doi: 10.18063/ijb.v6i3.270

109. de Melo BAG, Jodat YA, Cruz EM, *et al.*, 2020, Strategies to use fibrinogen as bioink for 3D bioprinting fibrin-based soft and hard tissues. *Acta Biomater*, 117: 60–76.

http://doi:10.1016/j.actbio.2020.09.024

110. Zhou Z, Cui J, Wu S, *et al.*, 2022, Silk fibroin-based biomaterials for cartilage/osteochondral repair. *Theranostics*, 12(11): 5103–5124.

http://doi:10.7150/thno.74548

111. Murphy SV, Atala A, 2014, 3D bioprinting of tissues and organs. *Nat Biotechnol,* 32(8): 773–785.

http://doi:10.1038/nbt.2958

112. Hölzl K, Lin S, Tytgat L, *et al.*, 2016, Bioink properties before, during and after 3D bioprinting. *Biofabrication*, 8(3): 032002.

http://doi:10.1088/1758-5090/8/3/032002

113. Hinton TJ, Jallerat Q, Palchesko RN, *et al.*, 2015, Three-dimensional printing of complex biological structures by freeform reversible embedding of suspended hydrogels. *Sci Adv,* 1(9): 1500758.

http://doi:10.1126/sciadv.1500758

114. Zhang J, Wehrle E, Adamek P, *et al.*, 2020, Optimization of mechanical stiffness and cell density of 3D bioprinted cell-laden scaffolds improves extracellular matrix mineralization and cellular organization for bone tissue engineering. *Acta Biomater*, 114: 307–322.

http://doi:10.1016/j.actbio.2020.07.016

115. Martyniak K, Lokshina A, Cruz MA, *et al.*, 2022, Biomaterial composition and stiffness as decisive properties of 3D bioprinted constructs for type II collagen stimulation. *Acta Biomater,* 152: 221–234.

http://doi:10.1016/j.actbio.2022.08.058

116. Allen NB, Abar B, Johnson L, *et al.*, 2022, 3D-bioprinted GelMA-gelatin-hydroxyapatite osteoblast-laden composite hydrogels for bone tissue engineering. *Bioprinting*, 26: e00196.

http://doi:10.1016/j.bprint.2022.e00196

117. Lee JS, Park HS, Jung H, *et al.*, 2020, Park, 3D-printable photocurable bioink for cartilage regeneration of tonsil-derived mesenchymal stem cells. *Addit Manuf,* 33: 101136.

http://doi:10.1016/j.addma.2020.101136

118. Bandyopadhyay A, Mandal BB, Bhardwaj N, 2022, 3D bioprinting of photo-crosslinkable silk methacrylate (SilMA)-polyethylene glycol diacrylate (PEGDA) bioink for cartilage tissue engineering. *J Biomed Mater Res Part A,* 110: 884–898.

http://doi:10.1002/jbm.a.37336

119. Rajput M, Mondal P, Yadav P, *et al.*, 2022, Light-based 3D bioprinting of bone tissue scaffolds with tunable mechanical properties and architecture from photocurable silk fibroin. *Int J Biol Macromol,* 202: 644–656.

http://doi:10.1016/j.ijbiomac.2022.01.081

120. Unagolla JM, Jayasuriya AC, 2020, Hydrogel-based 3D bioprinting: A comprehensive review on cell-laden hydrogels, bioink formulations, and future perspectives. *Appl Mater Today,* 18: 100479.

http://doi:10.1016/j.apmt.2019.100479

121. Koo Y, Choi E-J, Lee J, *et al.*, 2018, 3D printed cell-laden collagen and hybrid scaffolds for in vivo articular cartilage tissue regeneration. *J Ind Eng Chem,* 66: 343–355.

http://doi:10.1016/j.jiec.2018.05.049

122. Turnbull G, Clarke J, Picard F, *et al.*, 2018, 3D bioactive composite scaffolds for bone tissue engineering. *Bioact Mater,* 3: 278–314.

http://doi:10.1016/j.bioactmat.2017.10.001

123. Zhang B, Huang J, Narayan RJ, 2020, Gradient scaffolds for osteochondral tissue engineering and regeneration. *J Mater Chem B,* 8: 8149–8170.

http://doi:10.1039/D0TB00688B

124. Diaz-Gomez L, Kontoyiannis PD, Melchiorri AJ, *et al.*, 2019, Three-dimensional printing of tissue engineering scaffolds with horizontal pore and composition gradients. *Tissue Eng Part C Methods,* 25: 411–420.

http://doi:10.1089/ten.tec.2019.0112

125. Wang M, Li W, Mille LS, *et al.*, 2022, Digital light processing based bioprinting with composable gradients. *Adv Mater,* 34: 2107038.

http://doi:10.1002/adma.202107038

126. Nicolas J, Magli S, Rabbachin L, *et al.*, 2020, 3D extracellular matrix mimics: Fundamental concepts and role of materials chemistry to influence stem cell fate. *Biomacromolecules*, 21: 1968–1994.

http://doi:10.1021/acs.biomac.0c00045

127. Guvendiren M, Burdick JA, 2012, Stiffening hydrogels to probe short- and long-term cellular responses to dynamic mechanics. *Nat Commun*, 3: 792.

http://doi:10.1038/ncomms1792

128. Ji S, Almeida E, Guvendiren M, 2019, 3D bioprinting of complex channels within cell-laden hydrogels. *Acta Biomater* 95: 214–224.

http://doi:10.1016/j.actbio.2019.02.038

129. Martinez AW, Caves JM, Ravi S, *et al.*, 2014, Effects of crosslinking on the mechanical properties, drug release and cytocompatibility of protein polymers. *Acta Biomater*, 10: 26–33.

http://doi:10.1016/j.actbio.2013.08.029

130. FitzSimons TM, Anslyn EV, Rosales AM, 2022, Effect of pH on the properties of hydrogels cross-linked via dynamic thia-michael addition bonds. *ACS Polym Au,* 2: 129–136.

http://doi:10.1021/acspolymersau.1c00049

131. Bustamante-Torres M, Romero-Fierro D, Arcentales-Vera B, *et al.*, 2021, Hydrogels classification according to the physical or chemical interactions and as stimuli-sensitive materials. Gels, 7: 182.

http://doi:10.3390/gels7040182

132. Zhang YS, Khademhosseini A, 2017, Advances in engineering hydrogels. *Science*, 356: eaaf3627.

http://doi:10.1126/science.aaf3627

133. Lee J, Yeo M, Kim W, *et al.*, 2018, Development of a tannic acid cross-linking process for obtaining 3D porous cell-laden collagen structure. *Int J Biol Macromol,* 110: 497–503.

http://doi:10.1016/j.ijbiomac.2017.10.105

134. Ruedinger F, Lavrentieva A, Blume C, *et al.*, 2015, Hydrogels for 3D mammalian cell culture: a starting guide for laboratory practice. *Appl Microbiol Biotechnol,* 99: 623–636.

http://doi:10.1007/s00253-014-6253-y

135. Sang S, Mao X, Cao Y, *et al.*, 2023, 3D bioprinting using synovium-derived MSC-laden photo-cross-linked ECM bioink for cartilage regeneration. *ACS Appl Mater Interfaces*, 15: 8895–8913.

http://doi:10.1021/acsami.2c19058

136. Singh YP, Bandyopadhyay A, Mandal BB, 2019, 3D bioprinting using cross-linker-free silk–gelatin bioink for cartilage tissue engineering. *ACS Appl Mater Interfaces*, 11: 33684–33696.

http://doi:10.1021/acsami.9b11644

137. Kara Özenler A, Distler T, Tihminlioglu F, *et al.*, 2023, Fish scale containing alginate dialdehyde-gelatin bioink for bone tissue engineering. *Biofabrication*, 15: 025012.

http://doi:10.1088/1758-5090/acb6b7

138. Chakraborty J, Fernández-Pérez J, van Kampen KA, *et al.*, 2023, Development of a biomimetic arch-like 3D bioprinted construct for cartilage regeneration using gelatin methacryloyl and silk fibroin-gelatin bioinks. *Biofabrication*, 15: 035009.

http://doi:10.1088/1758-5090/acc68f

139. Chen P, Zheng L, Wang Y, *et al.*, 2019, Desktop-stereolithography 3D printing of a radially oriented extracellular matrix/mesenchymal stem cell exosome bioink for osteochondral defect regeneration. *Theranostics*, 9: 2439–2459.

http://doi:10.7150/thno.31017

140. Cidonio G, Alcala-Orozco CR, Lim KS, *et al.*, 2019, Osteogenic and angiogenic tissue formation in high fidelity nanocomposite Laponite-gelatin bioinks. *Biofabrication*, 11: 035027.

http://doi:10.1088/1758-5090/ab19fd

141. Irmak G, Gümüşderelioğlu M, 2020, Photo-activated platelet-rich plasma (PRP)-based patient-specific bio-ink for cartilage tissue engineering. *Biomed Mater,* 15: 065010.

http://doi:10.1088/1748-605X/ab9e46

142. Bai Z, Guo X-H, Tang C, *et al.*, 2018, Effects of artesunate on the expressions of insulin-like growth factor-1, osteopontin

and C-telopeptides of type II collagen in a rat model of osteoarthritis. *Pharmacology*, 101: 1–8.

http://doi:10.1159/000479160

143. Street J, Bao M, DeGuzman L, *et al.*, 2002, Vascular endothelial growth factor stimulates bone repair by promoting angiogenesis and bone turnover. *Proc Natl Acad Sci,* 99: 9656–9661.

http://doi:10.1073/pnas.152324099

144. Mi L, Liu H, Gao Y, *et al.*, 2017, Injectable nanoparticles/hydrogels composite as sustained release system with stromal cell-derived factor-1α for calvarial bone regeneration. *Int J Biol Macromol,* 101: 341–347.

http://doi:10.1016/j.ijbiomac.2017.03.098

145. Fujioka-Kobayashi M, Ota MS, Shimoda A, *et al.*, 2012, Cholesteryl group- and acryloyl group-bearing pullulan nanogel to deliver BMP2 and FGF18 for bone tissue engineering. *Biomaterials*, 33: 7613–7620.

http://doi:10.1016/j.biomaterials.2012.06.075

146. Fahimipour F, Dashtimoghadam E, Mahdi Hasani-Sadrabadi M, *et al.*, 2019, Enhancing cell seeding and osteogenesis of MSCs on 3D printed scaffolds through injectable BMP2 immobilized ECM-Mimetic gel. *Dent Mater,* 35: 990–1006.

http://doi:10.1016/j.dental.2019.04.004

147. Groll J, Burdick JA, Cho D-W, *et al.*, 2018, A definition of bioinks and their distinction from biomaterial inks. *Biofabrication*, 11: 013001.

http://doi:10.1088/1758-5090/aaec52

148. Colombo M, Bianchi A, 2010, Click chemistry for the synthesis of RGD-containing integrin ligands. *Molecules*, 15: 178–197.

http://doi:10.3390/molecules15010178

149. Panwar A, Tan L, 2016, Current status of bioinks for micro-extrusion-based 3D bioprinting. *Molecules*, 21: 685.

http://doi:10.3390/molecules21060685

150. Byambaa B, Annabi N, Yue K, *et al.*, 2017, Bioprinted osteogenic and vasculogenic patterns for engineering 3D bone tissue. *Adv Healthc Mater,* 6: 1700015.

http://doi:10.1002/adhm.201700015

151. Wang B, Díaz-Payno PJ, Browe DC, *et al.*, 2021, Affinity-bound growth factor within sulfated interpenetrating network bioinks for bioprinting cartilaginous tissues. *Acta Biomater,* 128: 130–142.

http://doi:10.1016/j.actbio.2021.04.016

152. Xie M, Wu D, Li G, *et al.*, 2021, Exosomes targeted towards applications in regenerative medicine. *Nano Sel,* 2: 880–908.

http://doi:10.1002/nano.202000251

153. Zhou Q, Cai Y, Lin X, 2020, The dual character of exosomes in osteoarthritis: Antagonists and therapeutic agents. *Acta Biomater,* 105: 15–25.

http://doi:10.1016/j.actbio.2020.01.040

154. Isaeva EV, Beketov EE, Demyashkin GA, *et al.*, 2022, Cartilage formation in vivo using high concentration collagen-based bioink with MSC and decellularized ECM granules. *Int J Mol Sci,* 23: 2703.

http://doi:10.3390/ijms23052703

155. Marcu IC, Illaste A, Heuking P, *et al.*, 2015, Functional characterization and comparison of intercellular communication in stem cell-derived cardiomyocytes. *Stem Cells*, 33: 2208–2218.

http://doi:10.1002/stem.2009

156. Tang J, Peng R, Ding J, 2010, The regulation of stem cell differentiation by cell-cell contact on micropatterned material surfaces. *Biomaterials*, 31: 2470–2476.

http://doi:10.1016/j.biomaterials.2009.12.006

157. Xu F, Sridharan B, Wang S, *et al.*, 2011, Embryonic stem cell bioprinting for uniform and controlled size embryoid body formation. *Biomicrofluidics*, 5: 022207.

http://doi:10.1063/1.3580752

158. Bourget J-M, Kérourédan O, Medina M, *et al.*, 2016, Patterning of endothelial cells and mesenchymal stem cells by laser-assisted bioprinting to study cell migration. *Biomed Res Int,* 2016: 1–7.

http://doi:10.1155/2016/3569843

159. Kolesky DB, Truby RL, Gladman AS, *et al.*, 2014, 3D bioprinting of vascularized, heterogeneous cell-laden tissue constructs. *Adv Mater,* 26: 3124–3130.

http://doi:10.1002/adma.201305506

160. Jakus AE, Rutz AL, Shah RN, 2016, Advancing the field of 3D biomaterial printing. *Biomed Mater,* 11: 014102.

http://doi:10.1088/1748-6041/11/1/014102

161. Ovsianikov A, James Y, Vladimir M, 2018, 3D printing and biofabrication. Springer International Publishing.

162. Morgan FLC, Moroni L, Baker MB, 2020, Dynamic bioinks to advance bioprinting. *Adv Healthc Mater,* 9: 1901798.

http://doi:10.1002/adhm.201901798

163. Nicodemus GD, Bryant SJ, 2008, Cell encapsulation in biodegradable hydrogels for tissue engineering applications. *Tissue Eng Part B Rev,* 14: 149–165.

http://doi:10.1089/ten.teb.2007.0332

164. Li H, Tan C, Li L, 2018, Review of 3D printable hydrogels and constructs. *Mater Des,* 159: 20–38.

http://doi:10.1016/j.matdes.2018.08.023

165. Mu X, Agostinacchio F, Xiang N, *et al.*, 2021, Recent advances in 3D printing with protein-based inks. *Prog Polym Sci,* 115: 101375.

http://doi:10.1016/j.progpolymsci.2021.101375

166. Simorgh S, Milan PB, Saadatmand M, *et al.*, 2021, Human olfactory mucosa stem cells delivery using a collagen hydrogel: As a potential candidate for bone tissue engineering. *Materials (Basel)*, 14: 1–17.

http://doi:10.3390/ma14143909

167. Wu X, Rapoport TA, 2018, Mechanistic insights into ER-associated protein degradation. *Curr Opin Cell Biol,* 53: 22–28.

http://doi:10.1016/j.ceb.2018.04.004

168. Verbeek CJR, van den Berg LE, 2010, Extrusion processing and properties of protein-based thermoplastics. *Macromol Mater Eng,* 295(1): 10–21.

http://doi:10.1002/mame.200900167

169. Rutz AL, Lewis PL, Shah RN, 2017, Toward next-generation bioinks: Tuning material properties pre- and post-printing to optimize cell viability. *MRS Bull,* 42(8): 563–570.

http://doi:10.1557/mrs.2017.162

170. Kabirian F, Mozafari M, 2020, Decellularized ECM-derived bioinks: Prospects for the future. *Methods*, 171: 108–118.

http://doi:10.1016/j.ymeth.2019.04.019

171. Pugliese R, Beltrami B, Regondi S, *et al.*, 2021, Polymeric biomaterials for 3D printing in medicine: An overview. *Ann 3D Print Med*, 2: 100011.

http://doi:10.1016/j.stlm.2021.100011

172. Parker ST, Domachuk P, Amsden J, *et al.*, 2009, Biocompatible silk printed optical waveguides. *Adv Mater,* 21: 2411–2415.

http://doi:10.1002/adma.200801580

173. Ramesh S, Harrysson OLA, Rao PK, *et al.*, 2021, Extrusion bioprinting: Recent progress, challenges, and future opportunities. *Bioprinting*, 21: e00116.

http://doi:10.1016/j.bprint.2020.e00116

174. Bedell ML, Navara AM, Du Y, *et al.*, 2020, Polymeric systems for bioprinting. *Chem Rev,* 120(19): 10744–10792.

http://doi:10.1021/acs.chemrev.9b00834

175. Chakraborty J, Mu X, Pramanick A, *et al.*, 2022, Recent advances in bioprinting using silk protein-based bioinks. *Biomaterials*, 287: 121672.

http://doi:10.1016/j.biomaterials.2022.121672

176. Zhou J, Zhang B, Shi L, *et al.*, 2014, Regenerated silk fibroin films with controllable nanostructure size and secondary structure for drug delivery. *ACS Appl Mater Interfaces*, 6(24): 21813–21821.

http://doi:10.1021/am502278b

177. Nikoomanzari E, Karbasi M, Melo WCMA, *et al.*, 2022, Impressive strides in antibacterial performance amelioration of Ti-based implants via plasma electrolytic oxidation (PEO): A review of the recent advancements. *Chem Eng J,* 441: 136003.

http://doi:10.1016/j.cej.2022.136003

178. Adhikari J, Roy A, Das A, *et al.*, 2021, Effects of processing parameters of 3D bioprinting on the cellular activity of bioinks. *Macromol Biosci,* 21(1): 2000179.

http://doi:10.1002/mabi.202000179

179. Hull SM, Brunel LG, Heilshorn SC, 2022, 3D bioprinting of cell-laden hydrogels for improved biological functionality. *Adv Mater*, 34(2): 2103691.

http://doi:10.1002/adma.202103691

180. Jaspe J, Hagen SJ, 2006, Do protein molecules unfold in a simple shear flow? *Biophys J,* 91(9): 3415–3424.

http://doi:10.1529/biophysj.106.089367

181. Nishioka GM, Markey AA, Holloway CK, 2004. Protein damage in drop-on-demand printers. *J Am Chem Soc*, 126(4): 16320–16321.

http://doi.org/10.1021/ja044539z

182. Delaney JT, Smith PJ, Schubert US, 2009, Inkjet printing of proteins. *Soft Matter,* 5(24): 4866–4877.

http://doi:10.1039/b909878j

183. Schwab A, Levato R, D'Este M, *et al.*, 2020, Printability and shape fidelity of bioinks in 3D bioprinting. *Chem Rev,* 120(19): 11028–11055.

http://doi:10.1021/acs.chemrev.0c00084

184. Neumann TV, Dickey MD, 2020, Liquid metal direct write and 3D printing: A review. *Adv Mater Technol,* 5(9): 2000070.

http://doi:10.1002/admt.202000070

185. Amorim PA, D'Ávila MA, Anand R, *et al.*, 2021, Insights on shear rheology of inks for extrusion-based 3D bioprinting. *Bioprinting*, 22: e00129.

http://doi:10.1016/j.bprint.2021.e00129

186. Joshi YM, Petekidis G, 2018, Yield stress fluids and ageing. *Rheol Acta,* 57(6-7): 521–549.

http://doi:10.1007/s00397-018-1096-6

187. Mouser VHM, Melchels FPW, Visser J, *et al.*, 2016, Yield stress determines bioprintability of hydrogels based on gelatin-methacryloyl and gellan gum for cartilage bioprinting. *Biofabrication*, 8(3): 035003.

http://doi:10.1088/1758-5090/8/3/035003

188. Sommer MR, Alison L, Minas C, *et al.*, 2017, 3D printing of concentrated emulsions into multiphase biocompatible soft materials. *Soft Matter,* 13(9): 1794–1803.

http://doi:10.1039/C6SM02682F

189. Nedunchezian S, Banerjee P, Lee C-Y, *et al.*, 2021, Generating adipose stem cell-laden hyaluronic acid-based scaffolds using 3D bioprinting via the double crosslinked strategy for chondrogenesis. *Mater Sci Eng C,* 124: 112072.

http://doi:10.1016/j.msec.2021.112072

190. Jiang Y, Zhou J, Feng C, *et al.*, 2020, Rheological behavior, 3D printability and the formation of scaffolds with cellulose nanocrystals/gelatin hydrogels. *J Mater Sci,* 55(33): 15709–15725.

http://doi:10.1007/s10853-020-05128-x

191. Bom S, Ribeiro R, Ribeiro HM, *et al.*, 2022, On the progress of hydrogel-based 3D printing: Correlating rheological properties with printing behaviour. *Int J Pharm,* 615: 121506.

http://doi:10.1016/j.ijpharm.2022.121506

192. Thattaruparambil Raveendran N, Vaquette C, Meinert C, *et al.*, 2019, Optimization of 3D bioprinting of periodontal ligament cells. *Dent Mater,* 35(12): 1683–1694.

http://doi:10.1016/j.dental.2019.08.114

193. Billiet T, Vandenhaute M, Schelfhout J, *et al.*, 2012, A review of trends and limitations in hydrogel-rapid prototyping for tissue engineering. *Biomaterials*, 33(26): 6020–6041.

http://doi:10.1016/j.biomaterials.2012.04.050

194. Nair K, Gandhi M, Khalil S, *et al.*, 2009, Characterization of cell viability during bioprinting processes. *Biotechnol J*, 4(8): 1168–1177.

http://doi:10.1002/biot.200900004

195. Chen DXB, 2019, Extrusion bioprinting of scaffolds, in *Extrusion Bioprinting of Scaffolds for Tissue Engineering Applications*, *Springer International Publishing*, Cham, 117–145.

http://doi:10.1007/978-3-030-03460-3_6

196. Daly AC, Freeman FE, Gonzalez-Fernandez T, *et al.*, 2017, 3D bioprinting for cartilage and osteochondral tissue engineering. *Adv Healthc Mater,* 6(22): 1–20.

http://doi:10.1002/adhm.201700298

197. Boularaoui S, Al Hussein G, Khan KA, *et al.*, 2020, An overview of extrusion-based bioprinting with a focus on induced shear stress and its effect on cell viability. *Bioprinting*, 20: e00093.

http://doi:10.1016/j.bprint.2020.e00093

198. Gu Q, Hao J, Lu Y, *et al.*, 2015, Three-dimensional bio-printing. *Sci China Life Sci,* 58(5): 411–419.

http://doi:10.1007/s11427-015-4850-3

199. Matai I, Kaur G, Seyedsalehi A, *et al.*, 2020, Progress in 3D bioprinting technology for tissue/organ regenerative engineering. *Biomaterials*, 226: 119536.

http://doi:10.1016/j.biomaterials.2019.119536

200. Di Bella C, Duchi S, O'Connell CD, *et al.*, 2018, In situ handheld three-dimensional bioprinting for cartilage regeneration. *J Tissue Eng Regen Med,* 12(3): 611–621.

http://doi:10.1002/term.2476

201. Xu T, Gregory C, Molnar P, *et al.*, 2006, Viability and electrophysiology of neural cell structures generated by the inkjet printing method. *Biomaterials,* 27(19): 3580–3588.

http://doi:10.1016/j.biomaterials.2006.01.048

202. Xu T, Jin J, Gregory C, *et al.*, 2005, Inkjet printing of viable mammalian cells. *Biomaterials,* 26(1): 93–99.

http://doi:10.1016/j.biomaterials.2004.04.011

203. Brenker JC, Devendran C, Neild A, *et al.*, 2020, On-demand sample injection: combining acoustic actuation with a tear-drop shaped nozzle to generate droplets with precise spatial and temporal control. *Lab Chip*, 20(2): 253–265.

http://doi:10.1039/C9LC00837C

204. Yang X, Lu Z, Wu H, *et al.*, 2018, Collagen-alginate as bioink for three-dimensional (3D) cell printing based cartilage tissue engineering. *Mater Sci Eng C,* 83: 195–201.

http://doi:10.1016/j.msec.2017.09.002

205. Lim H, Kim HS, Qazi R, *et al.*, 2020, Advanced soft materials, sensor integrations, and applications of wearable flexible hybrid electronics in healthcare, energy, and environment. *Adv Mater,* 32(15): 1901924.

http://doi:10.1002/adma.201901924

206. Slaughter BV, Khurshid SS, Fisher OZ, *et al.*, 2009, Hydrogels in regenerative medicine. *Adv Mater,* 21(32-33): 3307–3329.

http://doi:10.1002/adma.200802106

207. Fedorovich NEE, Alblas J, Hennink WEE, *et al.*, 2011, Organ printing: The future of bone regeneration? *Trends Biotechnol*, 29(12): 601–606.

http://doi:10.1016/j.tibtech.2011.07.001

208. Aldana AA, Abraham GA, 2017, Current advances in electrospun gelatin-based scaffolds for tissue engineering applications. *Int J Pharm*, 523(2): 441–453.

http://doi:10.1016/j.ijpharm.2016.09.044

209. Kim U-J, Park J, Li C, *et al.*, 2004, Structure and properties of silk hydrogels. *Biomacromolecules*, 5(3): 786–792.

http://doi:10.1021/bm0345460

210. Gupta S, Alrabaiah H, Christophe M, *et al.*, 2021, Evaluation of silk-based bioink during pre and post 3D bioprinting: A review. *J Biomed Mater Res Part B Appl Biomater,* 109(2): 279–293.

http://doi:10.1002/jbm.b.34699

211. Kim YB, Lee H, Kim GH, 2016, Strategy to achieve highly porous/biocompatible macroscale cell blocks, using a collagen/genipin-bioink and an optimal 3D printing process. *ACS Appl Mater Interfaces*, 8(47): 32230–32240.

http://doi:10.1021/acsami.6b11669

212. Chawla S, Midha S, Sharma A, *et al.*, 2018, Silk-based bioinks for 3D bioprinting. *Adv Healthc Mater,* 7(8): 1701204.

http://doi:10.1002/adhm.201701204

213. Kim BS, Das S, Jang J, *et al.*, 2020, Decellularized extracellular matrix-based bioinks for engineering tissue- and organ-specific microenvironments. *Chem Rev,* 120(19): 10608–10661.

http://doi:10.1021/acs.chemrev.9b00808

214. Bourgine PE, Pippenger BE, Todorov A, *et al.*, 2013, Tissue decellularization by activation of programmed cell death. *Biomaterials*, 34(19): 6099–6108.

http://doi:10.1016/j.biomaterials.2013.04.058

215. Groll J, Boland T, Blunk T, *et al.*, 2016, Biofabrication: Reappraising the definition of an evolving field. *Biofabrication*, 8(26): 013001.

http://doi:10.1088/1758-5090/8/1/013001

216. Sarkari S, Khajehmohammadi M, Davari N, *et al.*, 2022, The effects of process parameters on polydopamine coatings employed in tissue engineering applications. *Front Bioeng Biotechnol,* 10: 1005413.

http://doi:10.3389/fbioe.2022.1005413

217. Hong N, Yang G-H, Lee J, *et al.*, 2018, 3D bioprinting and its in vivo applications. *J Biomed Mater Res Part B Appl Biomater*, 106(1): 444–459.

http://doi:10.1002/jbm.b.33826

218. Ning L, Gil CJ, Hwang B, *et al.*, 2020, Biomechanical factors in three-dimensional tissue bioprinting. *Appl Phys Rev,* 7(4): 1–22.

http://doi:10.1063/5.0023206

219. Cui X, Boland T, 2009, Human microvasculature fabrication using thermal inkjet printing technology. *Biomaterials*, 30(31): 6221–6227.

http://doi:10.1016/j.biomaterials.2009.07.056

220. Gao G, Yonezawa T, Hubbell K, *et al.*, 2015, Inkjet-bioprinted acrylated peptides and PEG hydrogel with human mesenchymal stem cells promote robust bone and cartilage formation with minimal printhead clogging. *Biotechnol J,* 10(10): 1568–1577.

http://doi:10.1002/biot.201400635

221. Ihalainen P, Määttänen A, Sandler N, 2015, Printing technologies for biomolecule and cell-based applications. *Int J Pharm,* 494(2): 585–592.

http://doi:10.1016/j.ijpharm.2015.02.033

222. Pati F, Gantelius J, Svahn HA, 2016, 3D bioprinting of tissue/organ models. *Angew Chemie Int Ed,* 55(15): 4650–4665.

http://doi:10.1002/anie.201505062

223. Hong H, Seo YB, Kim DY, *et al.*, 2020, Digital light processing 3D printed silk fibroin hydrogel for cartilage tissue engineering. *Biomaterials*, 232: 119679.

http://doi:10.1016/j.biomaterials.2019.119679

224. Rice WL, Firdous S, Gupta S, *et al.*, 2008, Non-invasive characterization of structure and morphology of silk fibroin biomaterials using non-linear microscopy. *Biomaterials*, 29(13): 2015–2024.

http://doi:10.1016/j.biomaterials.2007.12.049

225. Tang S, Richardson BM, Anseth KS, 2021, Dynamic covalent hydrogels as biomaterials to mimic the viscoelasticity of soft tissues. *Prog Mater Sci,* 120: 100738.

http://doi:10.1016/j.pmatsci.2020.100738

226. Lim KS, Galarraga JH, Cui X, *et al.*, 2020, Fundamentals and applications of photo-cross-linking in bioprinting. *Chem Rev,* 120(19):10662–10694.

http://doi:10.1021/acs.chemrev.9b00812

227. Mueller E, Poulin I, Bodnaryk WJ, *et al.*, 2022, Click chemistry hydrogels for extrusion bioprinting: Progress, challenges, and opportunities. *Biomacromolecules*, 23(3): 619–640.

http://doi:10.1021/acs.biomac.1c01105

228. Rastin H, Ormsby RT, Atkins GJ, *et al.*, 2020, 3D bioprinting of methylcellulose/gelatin-methacryloyl (MC/GelMA) bioink with high shape integrity. *ACS Appl Bio Mater*, 3(3): 1815–1826.

http://doi:10.1021/acsabm.0c00169

229. GhavamiNejad A, Ashammakhi N, Wu XY, *et al.*, 2020, Crosslinking strategies for 3D bioprinting of polymeric hydrogels. *Small*, 16(35): 2002931.

http://doi:10.1002/smll.202002931

230. Gungor-Ozkerim PS, Inci I, Zhang YS, *et al.*, 2018, Bioinks for 3D bioprinting: An overview. *Biomater Sci,* 6(5): 915–946.

http://doi:10.1039/C7BM00765E

231. Hu W, Wang Z, Xiao Y, *et al.*, 2019, Advances in crosslinking strategies of biomedical hydrogels. *Biomater Sci,* 7(3): 843–855.

http://doi:10.1039/C8BM01246F

232. Lee JM, Suen SKQ, Ng WL, *et al.*, 2021, Bioprinting of collagen: Considerations, potentials, and applications. *Macromol Biosci,* 21(1): 1–18.

http://doi:10.1002/mabi.202000280

233. Zennifer A, Subramanian A, Sethuraman S, 2022, Bioprinting design considerations of bioinks for laser bioprinting technique towards tissue regenerative applications. *Bioprinting*, 27: e00205.

http://doi:10.1016/j.bprint.2022.e00205

234. Lin X, Tsao CT, Kyomoto M, *et al.*, 2022, Injectable natural polymer hydrogels for treatment of knee osteoarthritis. *Adv Healthc Mater*, 11(9): 2101479.

http://doi:10.1002/adhm.202101479

235. Zhao Q, Zhou Y, Wang M, 2021, Three-dimensional endothelial cell incorporation within bioactive nanofibrous scaffolds through concurrent emulsion electrospinning and coaxial cell electrospraying. *Acta Biomater,* 123: 312–324.

http://doi:10.1016/j.actbio.2021.01.035

236. Jung CS, Kim BK, Lee J, *et al.*, 2018. Development of printable natural cartilage matrix bioink for 3D printing of irregular tissue shape. *Tissue Eng Regen Med*, 15: 155–162.

https://doi.org/10.1007/s13770-017-0104-8

237. Visscher DO, Lee H, van Zuijlen PP, *et al.*, 2021. A photo-crosslinkable cartilage-derived extracellular matrix bioink for auricular cartilage tissue engineering. *Acta Biomater*, 121: 193–203.

https://doi.org/10.1016/j.actbio.2020.11.029